

Article

https://doi.org/10.1038/s41591-025-03692-w

Tand B cell responses against Epstein-Barr virus in primary sclerosing cholangitis

Received: 17 July 2024

Accepted: 31 March 2025

Published online: 11 June 2025



Hesham ElAbd®¹, Mitchell Pesesky®², Gabriel Innocenti³, Brian K. Chung⁴, Aya K. H. Mahdy¹, Valeriia Kriukova¹, Laila Kulsvehagen², Dennis Strobbe³, Claudia Stühler³, Gabriele Mayr¹, Damon H. May®², Melanie Prinzensteiner®³, Tim A. Steiert®¹, Florian Tran®¹, Michel V. Hadjihannas®¹, Rainer Günther³, Elisa Rosati®¹, Sören Mucha®¹o, Wolfgang Lieb¹o, Malte Ziemann®¹¹, Astrid Dempfle®¹², Felix Braun¹³, Trine Folseraas⁴,5,6, Johannes R. Hov®⁴,5,6, Espen Melum®⁴,5,6,1⁴, Petra Bacher¹,1⁵, Martina Sterneck¹6,1⁻, Tobias J. Weismüller®¹8,19, Henrike Lenzen²o, Bernd Bokemeyer²¹, Bryan Howie², Harlan S. Robins², Christoph Röcken®²², Stefan Schreiber®¹, Nina Khanna®³,2³, Anne-Katrin Pröbstel®¹,24,2⁵, Christoph Schramm®²6,27,28, Thomas Vogl³, Tom H. Karlsen®⁴,5,6 & Andre Franke®¹⊠

Primary sclerosing cholangitis (PSC) is an idiopathic, progressive and incurable liver disease. Here, we aimed for systematic analyses of adaptive immune responses in PSC. By profiling the T cell repertoires of 504 individuals with PSC and 904 healthy controls, we identified 1,008 clonotypes associated with PSC. A substantial fraction of these clonotypes was restricted to known PSC human leukocyte antigen susceptibility alleles and known to target Epstein–Barr virus (EBV) epitopes. We further utilized phage-immunoprecipitation sequencing to determine antibody epitope repertoires of 120 individuals with PSC and 202 healthy controls, which showed a higher burden of anti-EBV responses in PSC than controls. EBV-specific monoclonal antibodies isolated from B cells in PSC livers corroborated convergent B and T cell responses against EBV. By analyzing electronic health records of >116 million people, we identified an association between infectious mononucleosis and PSC (odds ratio, 12; 95% confidence interval, 6.3–22.9), suggesting a link between EBV and PSC.

PSC is characterized by chronic inflammation and progressive fibrosis of the bile ducts leading to bile duct obstruction and liver failure 1 . The lack of effective medical therapy means that liver transplantation is the only therapeutic option available in PSC with end-stage liver disease 1 . Although a rare disease with an incidence rate of -0.4 to 2.0 in 100,000 per year and a prevalence of 1 per 10,000 in the United States and Northern Europe, up to 10–15% of all liver transplantations in these regions can be attributed to PSC $^{2.3}$, and patient symptom burden and healthcare costs are high 4 . More than 30–40% of people with PSC

experience recurrence after liver transplantation despite the ongoing immunosuppression, sometimes requiring a second liver transplant, highlighting the need for a deeper understanding of disease etiology and effective treatments.

Several genetic variants at different loci show robust associations with PSC, for example, the T cell relevant *FOXP1* (ref. 5), *NFKB1* (ref. 6) and *CD226* (ref. 7) genes, in addition to multiple human leukocyte antigen (HLA) alleles, for example, HLA-B*08:01 and HLA-DRB1*13:01 (refs. 8,9). Direct evidence for an involvement of T cells has been

A full list of affiliations appears at the end of the paper. Me-mail: a.franke@ikmb.uni-kiel.de

reported, for example, an oligoclonal expansion of multiple T cell receptor (TCR) clonotypes in the bile duct in PSC was identified previously 10, indicating chronic antigenic exposure. Furthermore, an expansion of tissue-resident naive-like CD4 T cells in PSC livers has been reported Liver-infiltrating T cells exhibit functional differences, such as impaired proliferative activities 2, decreased production of IL-2, increased production of tumor necrosis factor and a reduction in CD28 surface expression 13, in PSC compared with controls. However, the antigenic targets of these liver-infiltrating T cells remain unknown.

TCRs govern the antigenic specificity of T cells and are generated through a somatic recombination process known as V(D)J recombination¹⁴ that creates a diverse repertoire of clonotypes, enabling T cells to recognize a wide range of antigens. Although recent advances in next-generation sequencing have enabled reliable identification of clonotypes^{15,16}, unraveling the corresponding antigen specificity remains difficult. Nonetheless, by comparing the TCR beta (TRB) repertoires of cytomegalovirus (CMV) seropositive and seronegative people statistically, clonotypes associated with CMV infection were identified¹⁷. The same framework was used to identify clonotypes associated with SARS-CoV-2 exposure¹⁸ and Lyme disease¹⁹. TCR profiling was also employed to discover clonotypes associated with chronic inflammatory diseases such as ankylosing spondylitis^{20,21}, enabling therapeutic strategies that deplete disease-associated clones and seem to introduce clinical remission in these patients²².

Here, we profiled the TRB repertoires of people with PSC using TCR sequencing (TCR-seq), which, relative to controls, showed distinct repertoire features, primarily expanded immune responses against several EBV epitopes. We then applied phage-immunoprecipitation sequencing (PhIP-seq)^{23,24} to profile antibody responses (from (1) blood and (2) monoclonal antibodies isolated from livers of people with PSC) against 357,000 bacterial and viral antigens, demonstrating converging expanded responses against EBV antigens in PSC.

Results

Identifying PSC-associated TRB clonotypes

Given the strong evidence for involvement of T cells in the pathogenesis of PSC, we profiled the TRB repertoires (Fig. 1a; Methods) of 504 individuals with PSC and 904 sex- and age-matched healthy controls (Extended Data Table 1). To identify PSC-associated clonotypes in a hypothesis-free manner, we compared their TRB repertoires with that of healthy controls (Methods)¹⁷, resulting in the identification of 136 clonotypes associated with PSC (Supplementary Table 1). We next expanded these 136 clonotypes into PSC-associated 'meta-clones' defined as a collection of highly similar clonotypes associated with PSC using seeded clustering (Methods). This enabled us to identify 1,008 PSC-associated clonotypes (Supplementary Table 2) arranged into 136 meta-clonotypes.

To validate the identified clonotypes, we analyzed their expansion in two independent cohorts. First, the 'A Study of a Prospective Adult Research Cohort with IBD' (SPARC IBD) cohort of the US-based Crohn's and Colitis Foundation inflammatory bowel disease (IBD) Plexus program²⁵ and, second, a PSC cohort from Norway (Methods). The SPARC IBD cohort contained 2,487 individuals with IBD only and 73 individuals with PSC-IBD. The identified 1,008 PSC-associated clonotypes were expanded significantly in people with PSC-IBD relative to IBD without PSC ($P=3.76\times10^{-5}$) (Extended Data Fig. 1a). Additionally, we compared the expansion of PSC-associated clonotypes in 154 people with PSC and 64 healthy controls from Norway, showing a significant expansion of these clonotypes in PSC ($P=1.16\times10^{-9}$) (Extended Data Fig. 1b).

To investigate whether PSC-associated clonotypes identified from blood were also present and/or expanded in affected PSC livers, we utilized a previously published dataset containing TRB repertoires of PSC livers²⁶ (Extended Data Fig. 2a). There was an overlap between PSC-associated clonotypes and PSC liver repertoires with a median of 12 PSC-associated clonotypes per repertoire. To investigate their

contribution to the blood compared with the liver repertoire, we utilized another previously published dataset²⁷ with paired blood and liver repertoires of people with PSC. Whereas the number of overlapping clonotypes was higher in blood than in liver biopsies (Extended Data Fig. 2b), the number of identified clonotypes in these two tissues, that is, the repertoire size, was different (Extended Data Fig. 2c). After normalizing by repertoire size, we observed a higher abundance of PSC-associated clonotypes in PSC livers relative to PSC-blood (Extended Data Fig. 2d). These findings indicate that the identified 1,008 PSC-associated clonotypes were not only expanded in blood but also in the liver of people with PSC, suggesting that these clonotypes may be involved in the ongoing liver pathology.

PSC-associated clonotypes are restricted to risk HLA alleles

Subsequently, we investigated the relationship between repertoire size and the number of PSC-associated clonotypes (n = 1,008), that is, the burden of PSC-associated clonotypes, which correlated poorly with repertoire size (Spearman correlation, -0.19; Fig. 1b). Additionally, the number of PSC-associated clonotypes per repertoire was higher in people with PSC relative to controls (P = 2.9 × 10⁻⁴³; Fig. 1c). To investigate factors shaping the burden of PSC-associated clonotypes, we normalized the burden of these clonotypes by repertoire size to produce a single number that represents the fraction of PSC-associated clonotypes in the repertoire. The normalized abundance did not correlate with the biological sex (Extended Data Fig. 3) or years since diagnosis (Extended Data Fig. 4). Given that conventional TCRs are restricted to particular HLA alleles, we tested whether differences in the HLA background of the study participants (Methods) might explain the difference in the normalized burden.

The alleles of the ancestral HLA haplotype 8.1 (AH 8.1) (HLA-(A*01:01, C*07:01, B*08:01, DRB1*03:01, DQA1*05:01 and DQB1*02:01)) were enriched in peoples with PSC compared with healthy controls (for example, for HLA-B*08:01, the frequency was 29% in PSC compared with 11% in controls; Extended Data Fig. 5). Given this strong association, we aimed to compare the normalized burden between carriers and noncarriers of these alleles, focusing on the two alleles with the strongest PSC association: HLA-B*08:01 (Fig. 1d) and HLA-DRB1*03:01 (Fig. 1e). The burden was dependent on two factors, the HLA background and disease status, with PSC carriers having the highest burden and noncarrier controls having the lowest. This finding suggests that PSC-associated meta-clonotypes represent public, HLA-restricted clonotypes that are present in carriers of AH 8.1 alleles but are significantly expanded in people with PSC relative to controls.

To discover the cognate HLA alleles of PSC-associated clonotypes, we queried the HLA-DB database²⁸. Out of the 1,008 PSC-associated clonotypes, 332 were observed in the HLA-DB. Of these, 87 were specific to HLA-B*08:01, 121 to HLA-DRB1*03:01, 21 to the HLA-DQA1*05:01-DQB1*02:01 heterodimer and 16 could not be distinguished between HLA-DRB1*03:01 and the HLA-DQA1*05:01-DQB1*02:01 heterodimer due to the strong linkage disequilibrium of the AH 8.1 haplotype (Fig. 2a). A smaller subset of clonotypes was also specific to HLA-DRB1*13:01—another known PSC risk allele (Fig. 2a). There were also several clusters without any known HLA association (Fig. 2a), these clonotypes might be restricted to HLA alleles that are rarer in the United States where the HLA-DB²⁸ was developed. Alternatively, they might be recognizing antigens that are not encountered at high frequency in healthy people and hence absent from the HLA-DB.

Next, we investigated common motifs within PSC-associated clonotype clusters (Fig. 2a). We started by analyzing the two main clusters that harbored multiple HLA-DRB1*03:01-restricted clonotypes. These clusters were defined by a clear motif that varied only in three (Fig. 2b) or two (Fig. 2c) amino acid sites. A similar pattern was observed for the two main clusters containing several HLA-B*08:01-restricted clonotypes (Fig. 2d,e). The complementarity-determining region

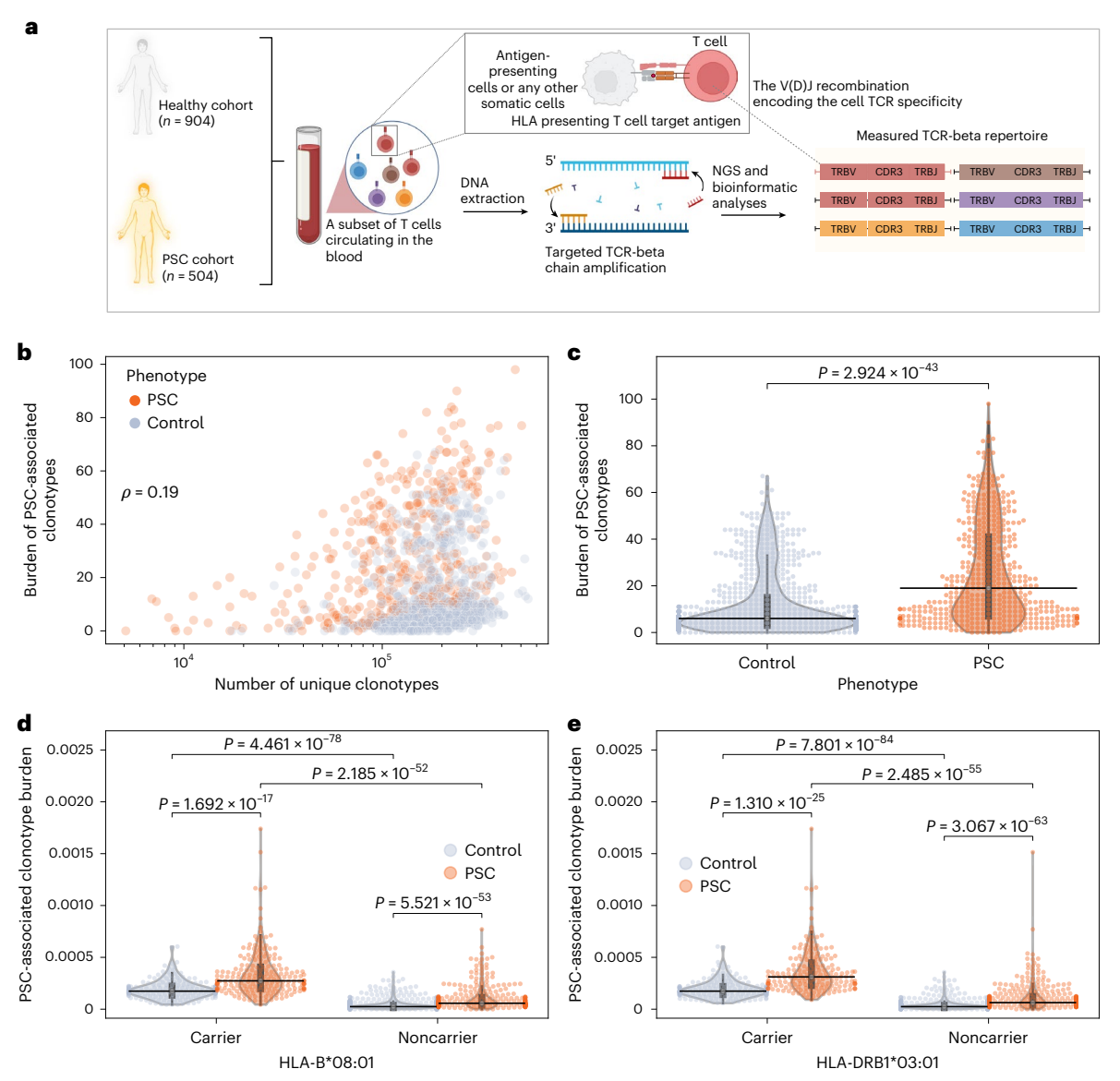


Fig. 1| Burden of PSC-associated meta-clonotypes and associations with alleles of the ancestral HLA haplotype 8.1. a, Schematic overview of the TCR sequencing (TCR-seq) pipeline used, starting with the collection of peripheral blood, followed by DNA extraction, then targeted amplification using PCR and then sequencing. Finally, different bioinformatic pipelines were used to identify T cell clonotypes and to quantify their expansion from the generated sequencing reads. b, Weak correlation between the burden of primary sclerosing cholangitis (PSC)-associated meta-clonotypes (n=1,008 clonotypes) and repertoire size as measured by Spearman correlation (ρ) across all repertoires (n=1,408 people). Burden is defined as the number of unique PSC-associated clonotypes identified in the repertoire of each person (y axis). The x axis shows the total number of unique clonotypes, defined as unique V and J genes combinations in addition to the amino acid sequence of the CDR3 region. c, Average difference in the burden

of PSC-associated meta-clonotypes in people with PSC (n=504) and controls (n=904). **d**, Normalized burden in HLA-B*08:01 carrier individuals with (n=205) and without (n=167) PSC relative to noncarrier individuals with (n=299) and without (n=737) PSC. **e**, The same observations for HLA-DRB1*03:01 carrier individuals with (n=179) and without (n=173) PSC in comparison with noncarrier individuals with (n=325) and without (n=731) PSC. In **b-e** each dot represents the repertoire of an individual with or without PSC; black lines represent the median across different individuals; boxplot, interquartile range (IQR); whiskers represent datapoints within the 1.5 times the IQR range. In **c-e**, a two-sided Mann–Whitney–Wilcoxon test was used to compare the burden or the normalized burden between the different groups included in the study. Panel **a** was created using BioRender.com.

3 (CDR3) amino acid motif for the biggest cluster without a known HLA allele (Fig. 2f) showed high sequence similarity to one of the HLA-B*08:01-restricted clusters (Fig. 2e). By comparing the V and J gene usages among the two clusters, we found that clonotypes derived from the unknown cluster (Fig. 2f) belong to the *TCRBV*07* gene family whereas the HLA-B*08:01-restricted cluster (Fig. 2e) contains *TCRBV*07:02*-derived clonotypes. This suggested that clonotypes derived from these two clusters (Fig. 2d,f) were probably a single cluster restricted to HLA-B*08:01 and are potentially responding to the same antigen. Thus, even though we identified over 1,008 PSC-associated

clonotypes, several of these clonotypes were restricted to known PSC risk alleles and shared a considerable degree of sequence similarity, suggesting that they recognize a limited set of antigens.

PSC-associated clonotypes recognize mainly EBV antigens

Subsequently, we sought to identify the antigen-specificity of PSC-associated clonotypes. First, we investigated the overlap between these clonotypes and public datasets, namely VDJdb²⁹ and McPAS-TCR³⁰. Given that most PSC-associated meta-clonotypes have been observed only rarely in public datasets, we focused on the main

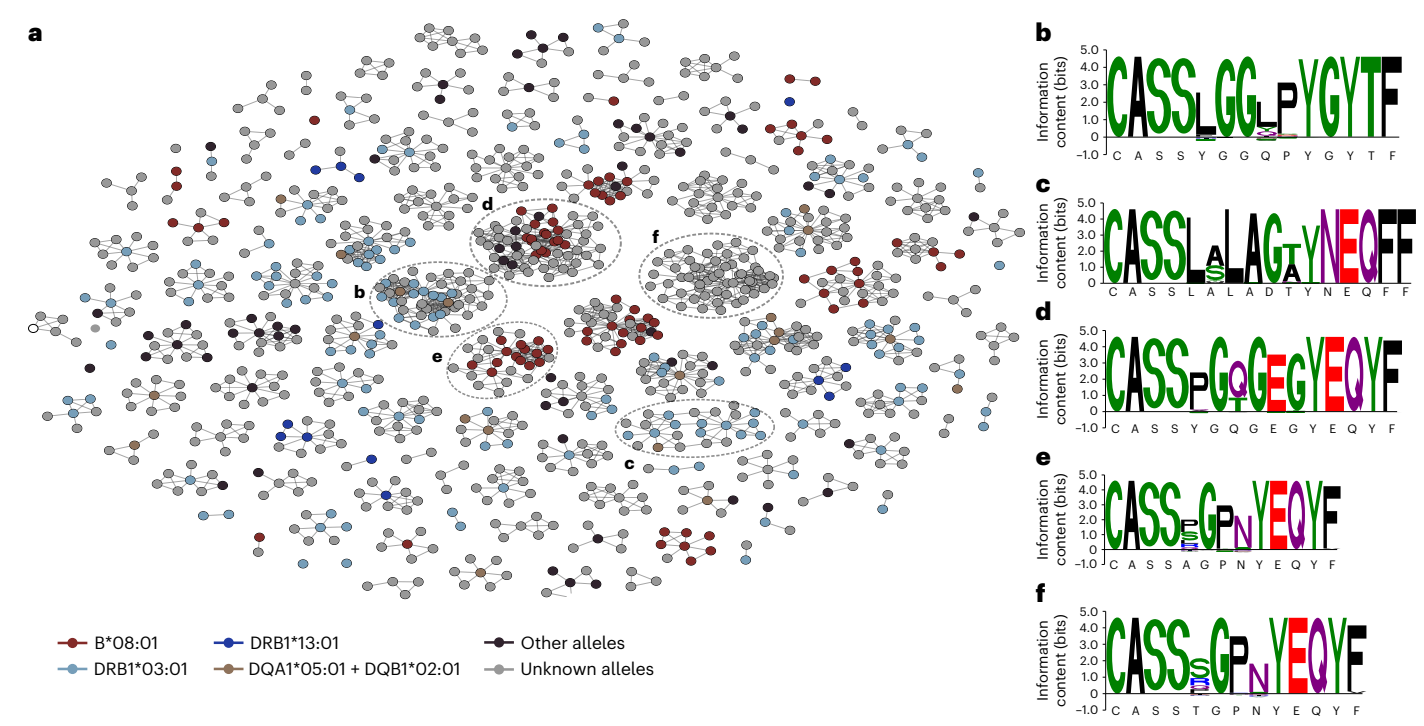


Fig. 2| **PSC-associated clonotypes are restricted to PSC risk HLA alleles. a**, Arrangement of primary sclerosing cholangitis (PSC)-associated clonotypes into several clusters. To build these clusters, we established an edge between two clonotypes (nodes in the graphic above) if the two clonotypes share the same V and J genes and differ in their complementarity-determining region 3 (CDR3) sequence by one amino acid only. **b,c**, The CDR3 motifs of the two main clusters associated with the HLA-DRB1*03:01 allele. Each of these clusters is derived from a different V/J gene combination and exhibits different CDR3 sequence

motif depicted in (**b**) and (**c**). **d**,**e**, Two main CDR3 motifs associated with the HLA-B*08:01 allele each with a distinct V/J gene usage and a CDR3 sequence. **f**, Motif derived from the largest cluster without a known HLA restriction. In **b-f**, amino acids are colored according to their physiochemical properties, whereas the height of each amino acid representation can be interpreted as the degree of conservation of a specific amino acid at a specific position within a CDR3 motif.

136 clonotypes identified before seeded clustering (Supplementary Table 1). Clonotypes were annotated with their antigenic target if they had a match in the database with the exact V and J gene as well as CDR3 amino acid sequence. The overlapping TRB clonotypes (n=12) were specific towards common pathogens such as EBV (n=6), CMV (n=3) and *Mycobacterium tuberculosis* (n=1). Given that the entries per pathogen in public databases vary, we calculated an enrichment P value using a hypergeometric test as employed in traditional gene enrichment analyses (Methods). As seen in Fig. 3a, only EBV-specific TRB clonotypes were enriched in people with PSC relative to controls ($P=9.96 \times 10^{-4}$).

We also queried a peptide-TCR interaction dataset that was generated using the MIRA assay³¹ and hosted by Adaptive Biotechnologies, which also showed an enrichment of EBV-specific clonotypes (Supplementary Table 3). Most of the clonotypes overlapping with the MIRA assay were known to recognize epitopes derived from the EBV lytic phase protein BZLF1 (n = 22 clonotypes out of 7,403 in the database) followed by the EBV latency III protein EBNA3 (n = 5 clonotypes out of 1,109 clonotypes) (Fig. 3b). To validate this experimentally, we enriched for EBV-specific TRB clonotypes using either HLA-B*08:01 tetramers loaded with peptides from the BZLF1 and EBNA3 proteins or using antigen stimulation with peptide pools derived from the BZLF1 and EBNA1 proteins followed by sorting of activated cells (Methods). Out of the 1,008 PSC-associated clonotypes we detected 13 clonotypes that overlapped with the sorted EBV-specific TRB clonotypes (n = 944), corroborating the in silico analyses. To further validate T cell recognition of EBV-infected B cells in an HLA-restricted manner in people with PSC, we assessed EBV-specific T cell reactivity using autologous and allogeneic HLA-B*08-matched EBV-transformed lymphoblastoid cell lines (LCLs) as well as untransformed B cells (Methods). Our findings revealed that PSC-derived T cell lines effectively recognized autologous LCLs (Extended Data Fig. 6). Additionally, we observed enhanced reactivity against LCLs compared with untransformed B cells when using allogeneic donor targets (Extended Data Fig. 6). To further characterize the disease-specific functionality of EBV-specific T cells in people with PCS, future studies will need to include healthy control samples and other disease controls.

We recently used co-occurrence clustering of common, HLA-associated clonotypes in 30,674 donor-repertoires to identify clonotype groupings that represent the public immune signature to common exposures (exposure co-occurrence clusters, hereafter referred to as ECOClusters), including EBV 32 . Utilizing co-occurrence clusters with our dataset, we identified 35 PSC-associated clonotypes in the previously determined 9,704 clonotypes EBV-specific ECOCluster was significantly higher in PSC relative to healthy controls ($P=2.97\times10^{-5}$; Fig. 3c). Thus, the co-occurrence analysis further supported the association of clonotypes specific to EBV in PSC and the link to known PSC HLA susceptibility alleles.

PSC-associated clonotypes are specifically expanded in PSC

To ensure that PSC-associated clonotypes were specific to PSC and not a general marker of liver injury, we calculated the normalized burden of PSC-associated clonotypes in other autoimmune liver diseases, that is, primary biliary cholangitis (PBC; n=63 repertoires) and autoimmune hepatitis (AIH; n=28 repertoires). The normalized burden was significantly higher in PSC relative to PBC samples ($P=1.6\times10^{-11}$) and AIH samples ($P=1.2\times10^{-2}$) (Fig. 3d). To exclude the possibility that PSC-associated clonotypes were confounded by concurrent IBD, which occurs in 60-80% of people with PSC¹, we determined the burden of

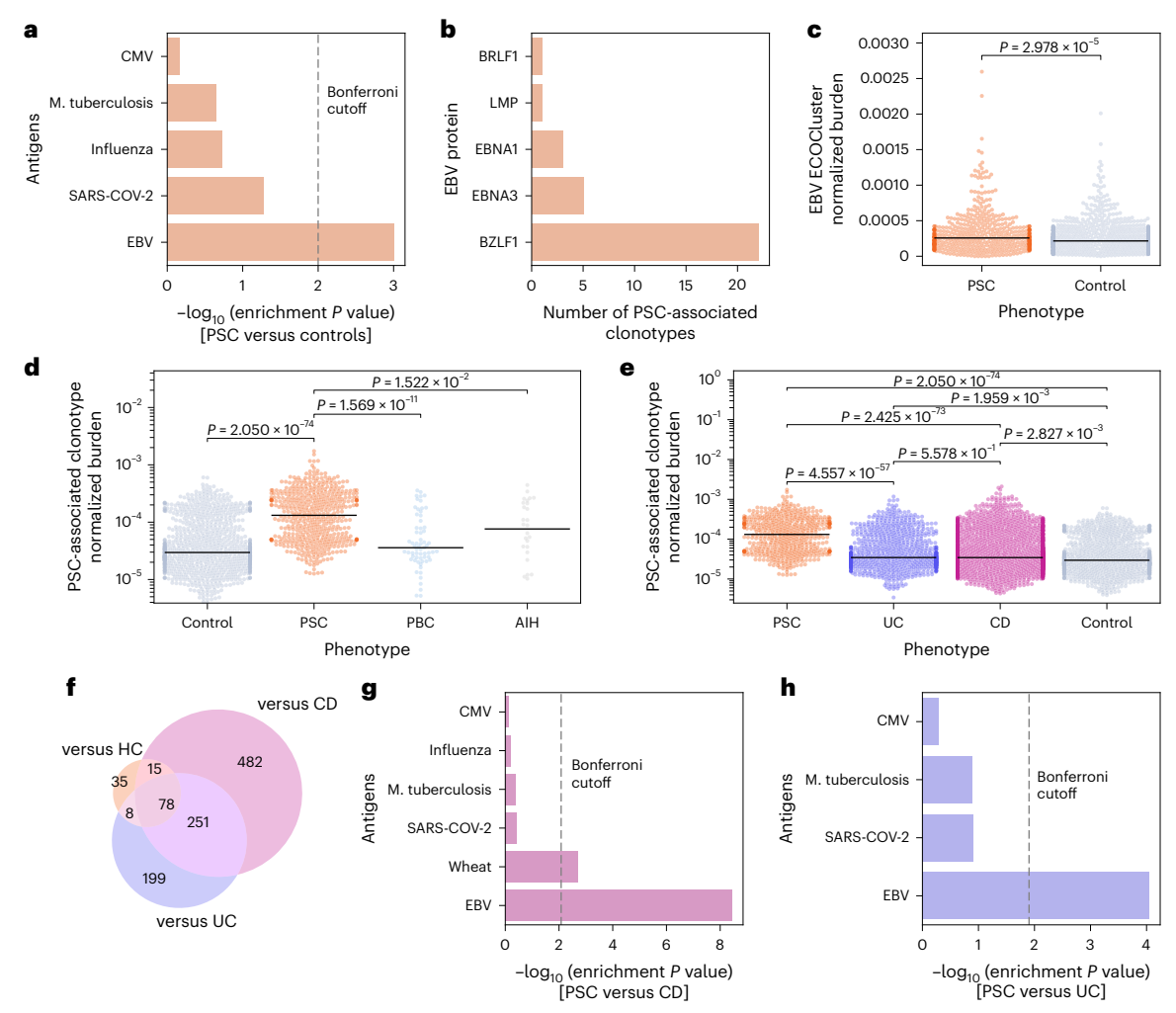


Fig. 3 | Pathogen enrichment analysis of PSC-associated clonotypes.

a, Enrichment of primary sclerosing cholangitis (PSC)-associated clonotypes identified by comparing the TCR beta (TRB) repertoires of people with PSC relative to controls. This enrichment analysis is based on the number of overlapping clonotypes, for example Epstein-Barr virus (EBV; n=6 clonotypes), cytomegalovirus (CMV; n=3 clonotypes) and M. tuberculosis (Mtb; n=1 clonotypes) and the number of pathogens-specific clonotypes in the public datasets. **b**, The strong response against the lytic phase master regulator BZLF1 protein of EBV obtained by searching the list of 1,008 PSC-associated clonotypes in the MIRA-generated annotation database (MIRA database); y axis, different EBV proteins; x axis, number of PSC-associated clonotypes that recognize peptides derived from these proteins. **c**, Burden of the EBV ECOCluster in people with PSC (n=504) and healthy controls (n=904). This burden was calculated by dividing the number of clonotypes overlapping with the EBV ECOCluster by the total number of clonotypes identified in a sample's repertoire. **d**, Difference in

the normalized burden of PSC-associated clonotypes (n = 1,008) in PSC relative to controls as well as two autoimmune liver diseases, namely primary biliary cholangitis (PBC; n = 63) and autoimmune hepatitis (AIH; n = 28). **e**, Burden of PSC-associated clonotypes in PSC relative to controls, people with Crohn's disease (CD; n = 2,037) and people with ulcerative colitis (UC; n = 844). **f**, Overlap in the sets of PSC-associated clonotypes identified by comparing the TRB repertoire of people with PSC with healthy controls (versus HC), people with UC (versus UC) and people with CD (versus CD). These sets of clonotypes were derived by comparing the different phenotypes, that is, CD, UC and controls with PSC. **g**, **h**, Pathogen enrichment analysis of PSC-associated clonotypes identified by comparing the TRB repertoire of people with PSC relative to people with CD (**g**) or UC (**h**). In **c**-**e**, each dot represents an individual, that is, the repertoire of a study participant, and black lines represent the median. All statistical comparisons were conducted using the two-sided Mann–Whitney–Wilcoxon test without correction for multiple testing.

these clonotypes in 2,037 people with Crohn's disease (CD) and 844 people with ulcerative colitis (UC), based on a recently described dataset³³. Again, the normalized burden of PSC-associated clonotypes was higher in PSC relative to UC ($P=4.5\times10^{-57}$) and CD ($P=2.4\times10^{-73}$) (Fig. 3e). Additionally, we compared the TRB repertoires of people with PSC with that of people with CD (n=2,037) and UC (n=844) using the approach used to identify PSC-associated clonotypes. Across the three comparisons, the same set of PSC-associated clonotypes were identified repeatedly (Fig. 3f). Subsequently, we ran a pathogen enrichment analysis on PSC-associated clonotypes identified from comparing PSC samples with either UC or CD, which showed that EBV-specific clonotypes were specifically enriched in PSC (versus CD, $P=3.71\times10^{-9}$ (Fig. 3g); versus UC, $P=9.1\times10^{-5}$ (Fig. 3h)). These findings suggest

that PSC-associated clonotypes were indeed specific to PSC and not shared with other chronic immune-mediated diseases of the liver and the bowel, such as PBC, AIH and IBD.

To investigate whether the expansion of PSC-associated clonotypes was different between people with PSC with and without IBD, that is, PSC and PSC-IBD, we compared the normalized burden of PSC-associated clonotypes among three groups, PSC (n=127 people), PSC-CD (n=33 people) and PSC-UC (n=167 people), showing no significant difference among these three groups. We next used the same statistical framework utilized for discovering PSC-associated clonotypes to discover clonotypes associated with each of these subphenotypes. Whereas there was a varying level of overlap among the associated clonotypes of the different subgroups, anti-EBV responses

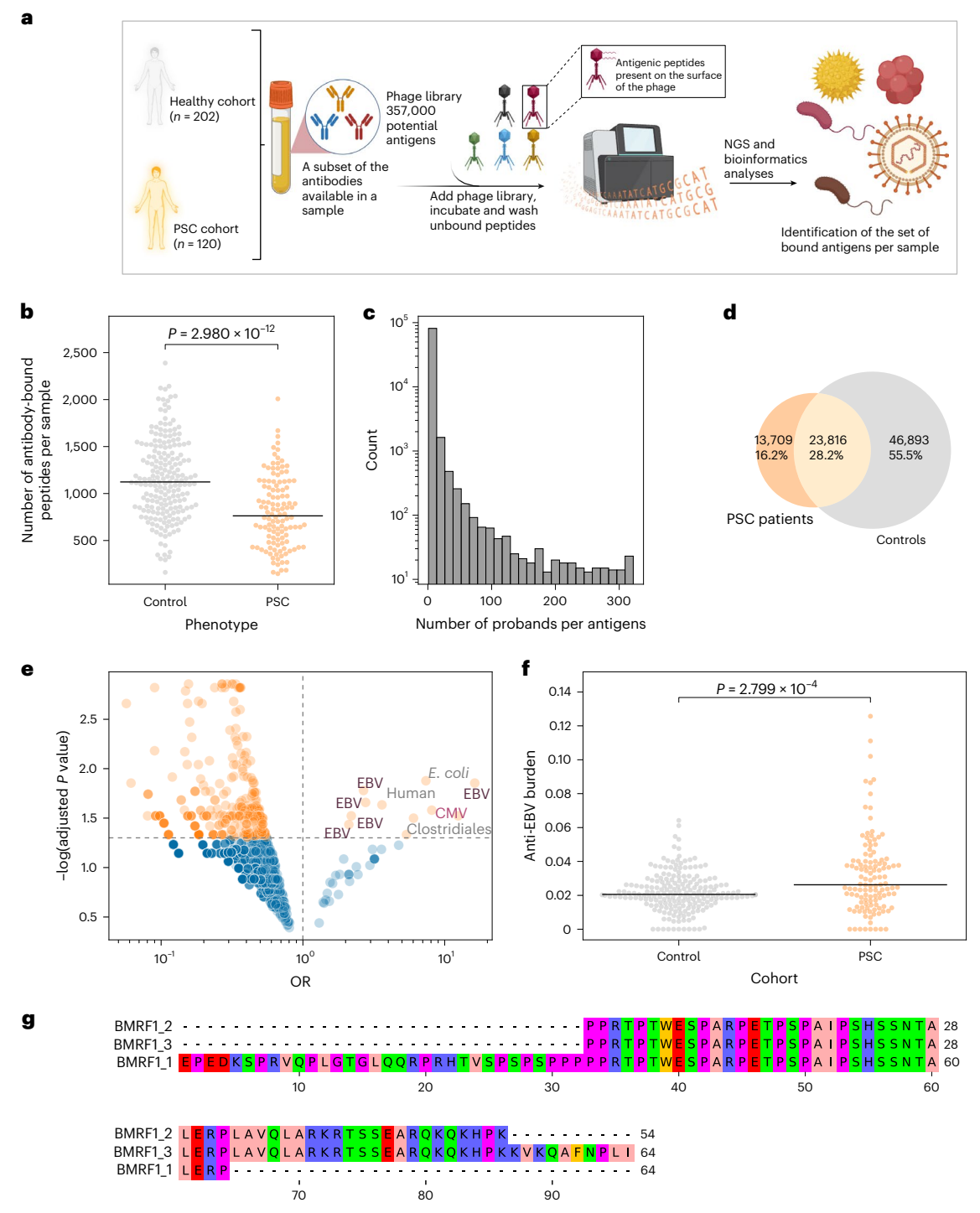


Fig. 4 | The antibody repertoire of people with PSC is marked by a higher burden of anti-EBV responses. a, Overview of the framework used to decode the exposure history of people with primary sclerosing cholangitis (PSC) and healthy controls using phage-immunoprecipitation sequencing (PhIP–seq). Briefly, sera were incubated with a bacteriophage library containing 357,000 peptides expressed on the capsids of the library bacteriophages. Subsequently, immunoprecipitation was conducted to pulldown antibody–bacteriophage complexes. After washing away unbound bacteriophages, DNA was extracted, and the inserted peptide sequences were amplified using PCR and then sequenced to identify target antigens that were recognized by the antibodies in the sera. b, Reduction in the number of bound antigens by the PSC cohort (n = 115) relative to controls (n = 201). c, Number of individuals binding to a particular antigen across all antigens included in the library. d, Number of antigens identified only in controls, in people with PSC or in both cohorts. e, Incidence analysis of antigens bound by the PSC and healthy cohorts; before

the analysis, we calculated the prevalence of each bound antigen in the PSC and healthy cohorts, and we restricted our analysis to antigens with an absolute difference in prevalence between the two cohorts of more than 0.05 (that is, 5% differences in prevalence between the two cohorts). ${\bf f}$, Burden of anti-Epstein-Barr virus (EBV) responses in the PSC cohort (n=115) relative to the healthy control cohort (n=201). The immune response burden was calculated by dividing the number of bound EBV antigens by the total number of antigens identified in the functional antibody repertoire. ${\bf g}$, The antigenic region of BMRF1, which is covered by three independent peptides identified from the incidence analysis shown in ${\bf e}$. In ${\bf g}$, the color scheme reflects the physicochemical properties of the amino acids. In ${\bf b}$ and ${\bf f}$, each dot represents an individual, that is, the repertoire of a study participant, and black lines represent the median. Additionally, the two-sided Mann–Whitney–Wilcoxon test was used to compare the functional antibody repertoire of people with PSC and healthy controls. Panel ${\bf a}$ was created using BioRender.com.

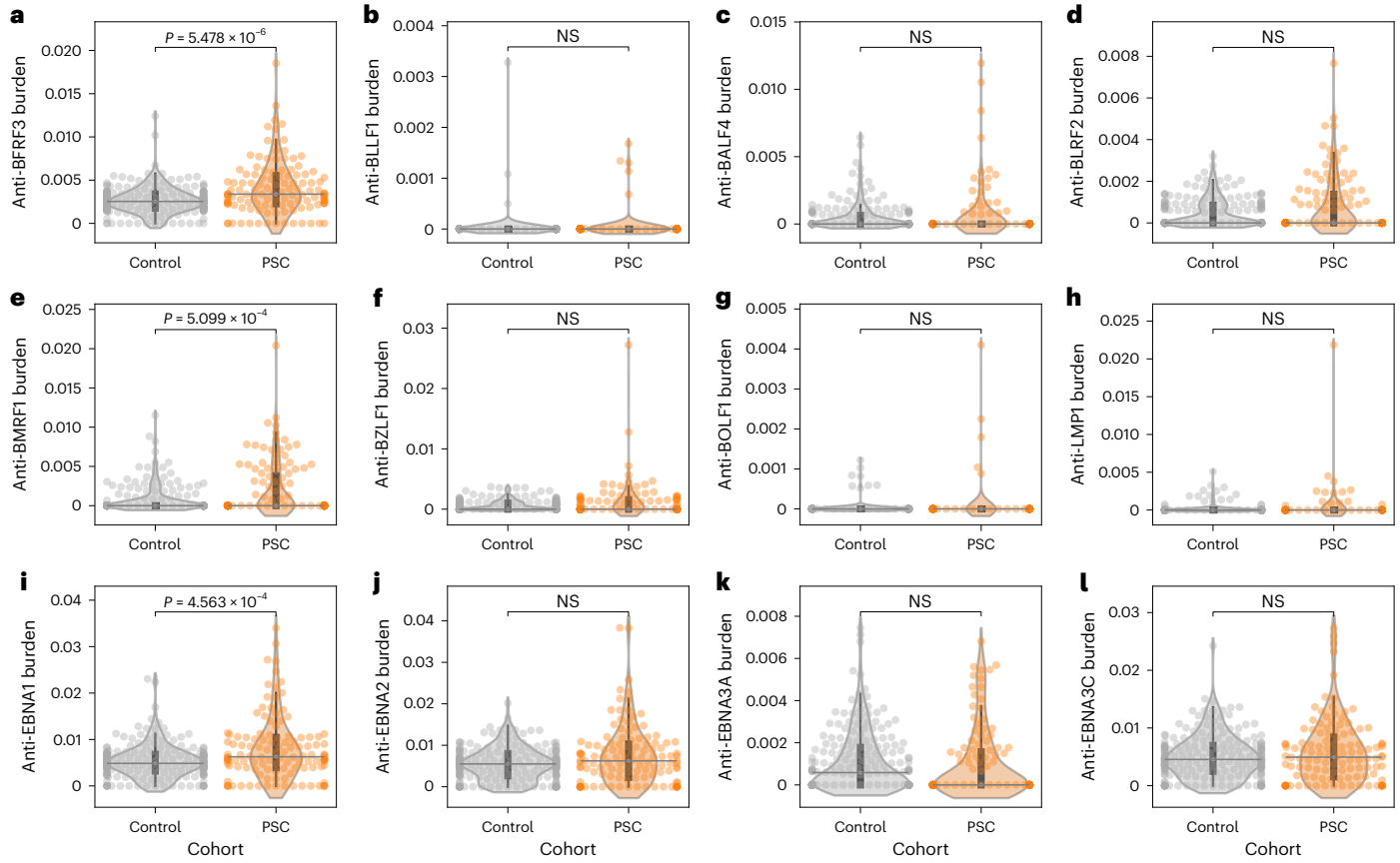


Fig. 5 | **Expansion of immune responses toward different EBV antigens in PSC and controls as inferred from PhIP-seq data.** In all panels, the burden of a particular protein in a sample refers to the number of antigens derived from this protein divided by the total number of antigens recognized in this sample, which was calculated for people with (n = 115) or without (n = 201) primary sclerosing cholangitis (PSC). a–d, Burden of capsid and structural Epstein-Barr virus (EBV) antigens, namely, BFRF3 (**a**), BLLF1 (**b**), BALF4 (**c**) and BLRF2 (**d**). **e–h**, Burden of lytic phase proteins, namely, BMRF1 (**e**), BZLF1 (**f**), BOLF1

 $\label{eq:continuous} \begin{tabular}{l} (g) and LMP1 (h). i-l Burden of different latency program antigens, namely EBNA1 (i), EBNA2 (j), EBNA3A (k) and EBNA3C (l). In all panels, each dot represents the burden of response against a particular EBV protein in an individual and black lines represent the median across different people, the boxplots represent the IQR and the whiskers represent datapoints within the 1.5 times the IQR range. All statistical comparisons were conducted using the two-sided Mann–Whitney–Wilcoxon test.$

were a common theme among these different clonotype sets. Specifically, five, 12 and four of the meta-clonotypes associated with PSC, PSC-UC and PSC-CD were EBV-specific, respectively. These findings indicate that elevated anti-EBV T cell responses are a common feature in PSC and its relevant subphenotypes.

Increased antibody responses against EBV in PSC

PhIP–seq enables the screening of antibody specificities by testing a predesigned subset, often several 100,000s, of peptides (antigens) against serum antibodies²⁴ of an individual. PhIP–seq has been used to understand factors shaping the immune response to different antigens^{34,35}, as well as for identifying the exposure signature of different diseases such as chronic fatigue syndrome³⁶ and inflammatory bowel disease³⁷.

To complement the results of the TCR profiling, and to analyze B cell responses, we performed PhIP–seq on sera from 202 healthy controls and 120 people with PSC, screening 357,000 peptides in parallel per serum sample (Fig. 4a). Relative to controls, PSC samples had a significantly lower number of bound antigens, that is, their serum antibodies recognized fewer antigens from the library relative to controls (Fig. 4b). Similar to previous PhIP–seq studies in other cohorts 34,35,37, most antigens in the library were detected in a single donor, that is, most responses were private (Fig. 4c).

Given the larger control sample size, most antigens were observed only in healthy controls (55%), with 16% only in people with PSC and 28%

in both PSC and matching controls (Fig. 4d). When we compared the prevalence, that is, the frequencies of recognized antigens in individuals with PSC versus healthy controls, using the Fisher's exact test, we observed a significantly higher prevalence in anti-EBV responses in people with PSC (Fig. 4e). We detected several overlapping antigens derived from the EBV protein BMRF1, also known as the early antigen diffuse component, which is a lytic phase protein (Fig. 4g). Globally, the fraction of anti-EBV responses relative to all bound antigens was significantly higher in people with PSC relative to controls (Fig. 4f). Thus, the PhIP–seq results complemented and corroborated the TCR analyses and showed that an expanded response towards EBV in PSC is evidenced for both T cells and B cells.

In PSC there is a robust EBV reactivation

Given the increased anti-EBV responses observed in people with PSC relative to controls, we investigated whether this is uniformly targeting all EBV antigens or is directed toward a subset of these antigens. Therefore, we compared antibody responses against different EBV antigens in people with PSC and controls, focusing on three groups of antigens defined in the utilized PhIP–seq library: (1) structural and capsid proteins, (2) lytic phase proteins and (3) latency phase proteins. Within the structural and capsid proteins group, only BFRF3 had a significantly higher burden in people with PSC relative to controls (Fig. 5a–d), and antibodies against BFRF3 were also shown to be cross-reactive to human proteins such as septin-9 (ref. 38). Within the

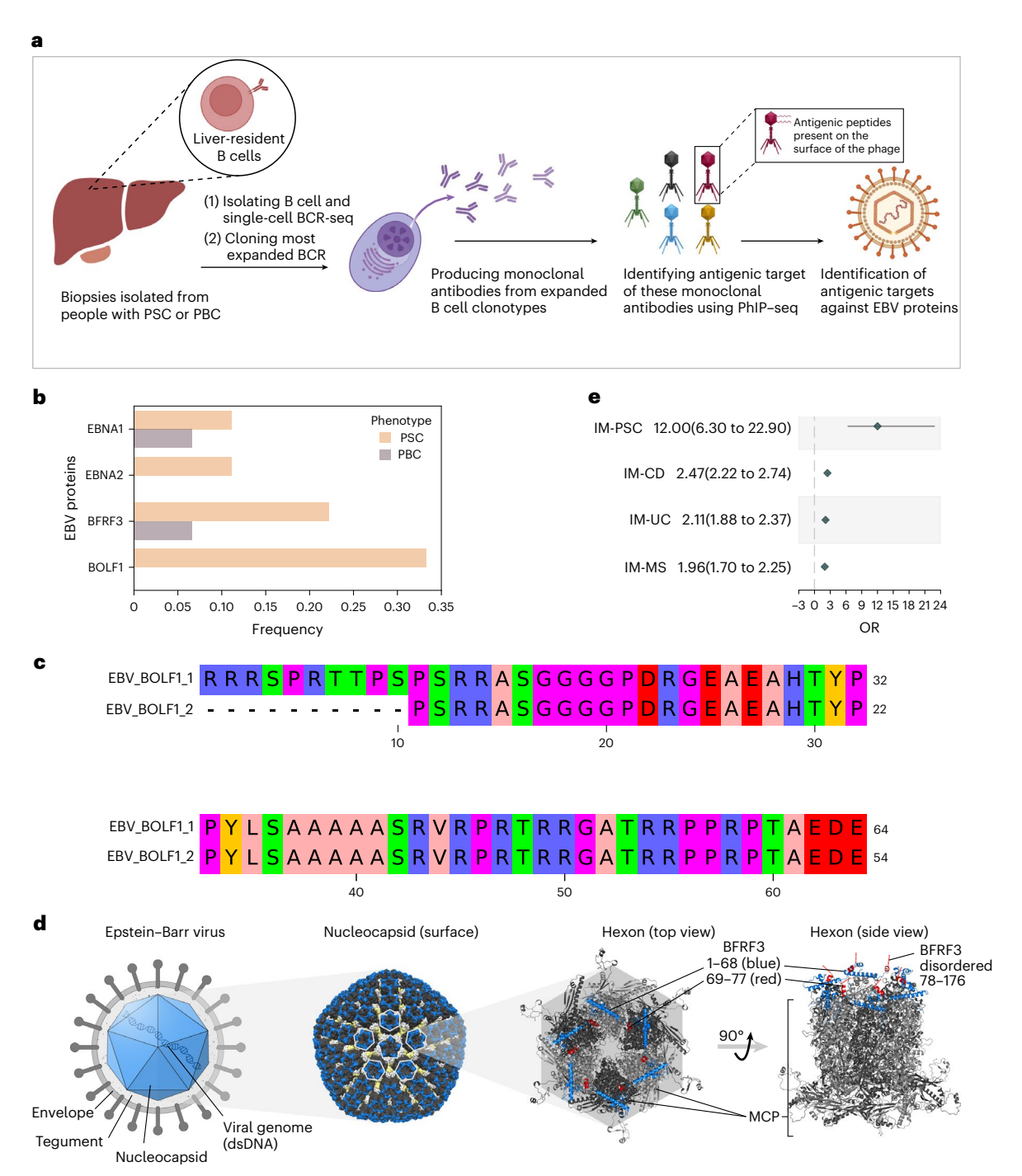


Fig. 6 | **Expanded liver-resident B** cells in people with PSC show a higher anti-EBV response burden relative to PBC. a, Steps used to generate monoclonal antibodies from liver-derived B cells and to decode their antigenic specificities. Briefly, single-cell B cell receptor sequencing was conducted on B cells isolated from liver biopsies. Subsequently, expanded B cell clonotypes were cloned into a mammalian expression system to produce monoclonal antibodies. The antigenic specificities of these monoclonal antibodies was identified using phage-immunoprecipitation sequencing (PhIP-seq). **b**, Frequency of anti-EBV monoclonal antibodies generated from expanded B cells in the liver of three PSC (*n* = 9 total antibodies) and three PBC liver biopsies (*n* = 15 total antibodies). Frequency was calculated across the produced monoclonal antibodies and not the number of samples. **c**, The antigenic region of BOLF1 to which monoclonal antibodies from the liver of people with PSC bind. **d**, Three-dimensional

location of BFRF3 (blue) on the surface of the EBV capsid structure. The capsid is composed of 11 pentons and 150 surrounding hexons 56 , which are complexes of several different proteins, among which a multimer of the main capsid protein (MCP, light and dark gray cartoons) provides for the main structural basis together with BFRF3 cross-linking on the top. BFRF3 also mediates Tegument binding through the flexible C terminus 56 . The antigenic peptide ranges from 69 to 122 and is partly structured (red helices, positions 69–77) but mostly disordered (indicated schematically as a thin red line). \mathbf{e} , Association of different autoimmune and immune-mediated inflammatory diseases, including primary sclerosing cholangitis (PSC), Crohn's disease (CD), ulcerative colitis (UC) and multiple sclerosis (MS) with infectious mononucleosis (IM), with filled diamonds representing the association odds ratio (OR) and error bars representing the 95% CI. Panel \mathbf{a} was created using BioRender.com.

lytic phase antigens, only BMRF1 had a significantly higher burden in PSC relative to controls (Fig. 5e-h). Within the subset of latency proteins (Fig. 5i-l), only EBNA1 had a higher response burden in people with PSC relative to controls (Fig. 5i).

We then used the PhIP-seq data to impute EBV seropositivity rates in people with PSC and controls using three EBV proteins: BMRF1 (early antigen diffuse component), EBNA1 and BFRF3 (part of the viral capsid antigen), defining positivity as having three bound antigens or more per protein. This resulted in an EBV seropositivity rate of 27.8% in people with PSC and 14.9% in controls based on BMRF1 (P = 0.008), 80.8% in PSC and 85% in controls based on EBNA1 (P = 0.34) and 74.7% in PSC and 67.6% in controls based on BFRF3 (P = 0.20). We also defined EBV-positivity as having a positive response toward any of these three proteins, resulting in a positivity rate of 90.4% in people with PSC and 91% in controls (P = 0.84). These data indicate that, in PSC, there was an elevated immune response toward lytic phase antigens, suggesting EBV reactivation in PSC similar to other autoimmune diseases such as rheumatoid arthritis (RA)³⁹, multiple sclerosis (MS)⁴⁰ and Sjögren syndrome⁴¹. Nonetheless, there is a small fraction of EBV-negative people with PSC, possibly due to phenotype heterogeneity (PSC-like conditions caused by other etiologies) or a reflection that PSC in rare cases may arise also in an EBV-negative setting.

Expanded B cells in PSC livers produce anti-EBV antibodies

We further investigated liver-infiltrating B cells in PSC by collecting liver biopsies from three people with PSC and three people with PBC (as a control group). Subsequently, we produced monoclonal antibodies from expanded B cells (Methods) and characterized their cognate antigens using PhIP-seq (Fig. 6a). Given the small sample size and building from our previous findings, we focused our analysis on EBV antigens, which were found to have a higher frequency in PSC relative to PBC livers (Fig. 6b). Due to the small sample size, we were not able to perform robust statistical testing to compare the frequency of EBV bound antigens between PSC and PBC samples. Nonetheless, antibodies that had higher abundance in the sera of people with PSC relative to controls were also detected at a higher frequency in PSC livers. These included antibodies against the small capsid protein (SCP/BFRF3) (Fig. 5a) as well as EBNA1 (Fig. 5i). We also observed antibody responses against two additional epitopes from the EBV lytic phase protein BOLF1 (Fig. 6c), corroborating our previous findings about the higher burden of anti-EBV responses in PSC relative to controls. Mapping the BFRF3 antigenic region bound by the monoclonal antibody present in PSC livers onto the three-dimensional structure of the protein pointed towards the partially disordered C-terminal region of the capsid protein as a key epitope (Fig. 6d).

Infectious mononucleosis is associated with PSC

To assess the epidemiological plausibility of our findings, we investigated a potential link between infectious mononucleosis, which is commonly caused by an EBV infection 42 , and PSC. To this end, we used the TriNetX database (Methods), containing >116 million electronic health records, to associate infectious mononucleosis with PSC (Fig. 6e). Infectious mononucleosis was associated significantly with PSC (odds ratio (OR) = 12; 95% confidence interval (Cl), 6.3–22.9), which was higher than for inflammatory bowel disease, specifically, CD (OR = 2.47; 95% CI, 2.22–2.74) and UC (OR = 2.11; 95% CI, 1.88–2.37), as well as for MS (OR = 1.96; 95% CI, 1.7–2.25). Overall, these findings support an immunological link between EBV and PSC.

Discussion

Using large-scale high-throughput immune-profiling technologies such as TCR-seq and PhIP-seq in addition to epidemiological data, we were able to establish a strong association between EBV and PSC. EBV has been implicated previously in multiple autoimmune diseases and immune-mediated inflammatory diseases⁴³ such as MS⁴⁴, RA³⁹, systemic lupus erythematosus (SLE)⁴⁵ and Sjögren syndrome⁴⁶. EBV

reactivation—a process where the virus exits its latency and starts its lytic program—has been observed in several autoimmune diseases, for example, SLE⁴⁷, RA³⁹ and in MS⁴⁰. We observed higher antibody responses against the BMRF1 protein and elevated T cell-mediated responses against the BZLF1 protein, both of which are lytic phase proteins, in people with PSC relative to healthy controls, suggesting that EBV reactivation is probably involved in the pathogenesis of PSC, similar to other autoimmune diseases⁴³.

Although the contribution of EBV and EBV reactivation in autoimmune diseases remains poorly understood, different mechanisms, such as molecular mimicry, have been proposed. Within SLE cross-reactivities between the EBNA1 protein and Ro60 (ref. 48) as well as Clq^{49} were observed, similarly, in MS between EBNA1 and GlicalCAM 50 . Here, we observed a significant increase in the anti-EBNA1 responses in people with PSC relative to controls. Whereas this may suggest the presence of a yet-to-be-discovered cross-reactive self-antigen in PSC, it could also indicate a dysregulated immune response toward EBV antigens. Specifically, viral proteins produced during viral replication can have immunomodulatory effects, for example, BZLF1 can inhibit INF γ signaling and the production of inflammatory cytokines 2. Additionally, BMRF1 inhibits responses to DNA damage 3 and BZLF1 interferes with the cell cycle to increase EBV viral production 2.

Although the molecular data provide evidence for the involvement of EBV in the pathophysiology of PSC, it does not establish a causal relationship between EBV and PSC due to the cross-sectional study design. Using temporal data from, for example, the Department of Defense Serum Repository 54 , a relationship between EBV infection before the onset of MS could be established 44 . Similar observations have also been recently made for IBD 55 . A common feature of these studies is the long timespan between EBV infection and the onset of these diseases. This suggests that multiple rounds of EBV reactivation, additional risk factors/triggers and/or a prolonged interaction between EBV and the host immune system are needed for disease development.

The TCR-seq analysis enabled us to identify TRB clonotypes that are expanded in people with PSC; however, it did not provide the functional state of T cells expressing these TRB chains, for example, their subtypes and gene expression patterns. Furthermore, most of the identified clonotypes were restricted to known HLA risk alleles, such as HLA-B*08:01 and HLA-DRB1*03:01, which are frequent in people with PSC but are not PSC specific. Whereas our PhIP-seq library covered multiple EBV epitopes, it did not cover the entire antigenic space of EBV: subsequently, only a subset of potential epitopes could be measured in the current study. Follow-up studies should focus on investigating the entire antigenic space of EBV using tailored libraries, and replication and elaboration of relevant antigenic specificities in diverse PSC cohorts from other geographical regions are warranted. Additionally, quantification of the EBV seropositivity rate in large PSC cohorts would be needed to further disentangle the role of EBV in the pathogenesis of PSC and recurrent PSC after liver transplantation.

In conclusion, our analysis has established a strong link between EBV infection and PSC. Further studies are needed to elucidate potential mechanisms by which infectious mononucleosis and EBV infection contribute to PSC development.

Online content

Any methods, additional references, Nature Portfolio reporting summaries, source data, extended data, supplementary information, acknowledgements, peer review information; details of author contributions and competing interests; and statements of data and code availability are available at https://doi.org/10.1038/s41591-025-03692-w.

References

 Karlsen, T. H., Folseraas, T., Thorburn, D. & Vesterhus, M. Primary sclerosing cholangitis; a comprehensive review. J. Hepatol. 67, 1298–1323 (2017).

- Carbone, M. et al. Liver transplantation for primary sclerosing cholangitis (PSC) with or without inflammatory bowel disease (IBD)—a European Society of Organ Transplantation (ESOT) consensus statement. *Transpl. Int.* 36, 11729 (2023).
- Chazouilleres, O. et al. EASL clinical practice guidelines on sclerosing cholangitis. J. Hepatol. 77, 761–806 (2022).
- van Munster, K. N. et al. Disease burden in primary sclerosing cholangitis in the Netherlands: a long-term follow-up study. *Liver Int.* 43, 639–648 (2023).
- Ji, S.-G. et al. Genome-wide association study of primary sclerosing cholangitis identifies new risk loci and quantifies the genetic relationship with inflammatory bowel disease. *Nat. Genet.* 49, 269–273 (2017).
- Ellinghaus, D. et al. Analysis of five chronic inflammatory diseases identifies 27 new associations and highlights disease-specific patterns at shared loci. *Nat. Genet.* 48, 510–518 (2016).
- Liu, J. Z. et al. Dense genotyping of immune-related disease regions identifies nine new risk loci for primary sclerosing cholangitis. Nat. Genet. 45, 670–675 (2013).
- Næss, S. et al. Refinement of the MHC risk map in a Scandinavian primary sclerosing cholangitis population. PLoS ONE 9, e114486 (2014).
- Karlsen, T. H. et al. Different HLA class II associations in ulcerative colitis patients with and without primary sclerosing cholangitis. Genes Immun. 8, 275–278 (2007).
- Probert, C. S. et al. Analysis of human common bile duct-associated T cells: evidence for oligoclonality, T cell clonal persistence, and epithelial cell recognition. *J. Immunol.* 158, 1941–1948 (1997).
- Poch, T. et al. Single-cell atlas of hepatic T cells reveals expansion of liver-resident naive-like CD4⁺ T cells in primary sclerosing cholangitis. J. Hepatol. 75, 414–423 (2021).
- Bo, X., Broome, U., Remberger, M. & Sumitran-Holgersson, S. Tumour necrosis factor α impairs function of liver derived T lymphocytes and natural killer cells in patients with primary sclerosing cholangitis. Gut 49, 131–141 (2001).
- Liaskou, E. et al. Loss of CD28 expression by liver-infiltrating T cells contributes to pathogenesis of primary sclerosing cholangitis. Gastroenterology 147, 221–232.e7 (2014).
- Roth, D. B. V(D)J recombination: mechanism, errors, and fidelity. *Microbiol. Spectr.* https://doi.org/10.1128/microbiolspec.MDNA3-0041-2014 (2014).
- Robins, H. Immunosequencing: applications of immune repertoire deep sequencing. *Curr. Opin. Immunol.* 25, 646–652 (2013).
- Carlson, C. S. et al. Using synthetic templates to design an unbiased multiplex PCR assay. Nat. Commun. 4, 2680 (2013).
- Emerson, R. O. et al. Immunosequencing identifies signatures of cytomegalovirus exposure history and HLA-mediated effects on the T cell repertoire. Nat. Genet. 49, 659–665 (2017).
- Snyder, T. M. et al. Magnitude and dynamics of the T-cell response to SARS-CoV-2 infection at both individual and population levels. Front. Immunol. https://doi.org/10.3389/fimmu.2024.1488860 (2025).
- Greissl, J. et al. Immunosequencing of the T-cell receptor repertoire reveals signatures specific for identification and characterization of early Lyme disease. Preprint at medRxiv https://doi.org/10.1101/2021.07.30.21261353 (2022).
- Komech, E. A. et al. CD8⁺ T cells with characteristic T cell receptor beta motif are detected in blood and expanded in synovial fluid of ankylosing spondylitis patients. *Rheumatology* 57, 1097–1104 (2018).
- 21. Faham, M. et al. Discovery of T cell receptor β motifs specific to HLA-B27-positive ankylosing spondylitis by deep repertoire sequence analysis. *Arthritis Rheumatol.* **69**, 774–784 (2017).

- Britanova, O. V. et al. Targeted depletion of TRBV9⁺ T cells as immunotherapy in a patient with ankylosing spondylitis. *Nat. Med.* 29, 2731–2736 (2023).
- 23. Larman, H. B. et al. Autoantigen discovery with a synthetic human peptidome. *Nat. Biotechnol.* **29**, 535–541 (2011).
- Mohan, D. et al. PhIP-seq characterization of serum antibodies using oligonucleotide-encoded peptidomes. *Nat. Protoc.* 13, 1958–1978 (2018).
- Raffals, L. E. et al. The development and initial findings of a study of a prospective adult research cohort with inflammatory bowel disease (SPARC IBD). *Inflamm. Bowel Dis.* 28, 192–199 (2022).
- Liaskou, E. et al. High-throughput T-cell receptor sequencing across chronic liver diseases reveals distinct disease-associated repertoires. Hepatology 63, 1608–19 (2016).
- Henriksen, E. K. K. et al. Gut and liver T-cells of common clonal origin in primary sclerosing cholangitis-inflammatory bowel disease. J. Hepatol. 66, 116–122 (2017).
- 28. Zahid, H. J. et al. Large-scale statistical mapping of T-cell receptor β sequences to human leukocyte antigens. Preprint at *bioRxiv* https://doi.org/10.1101/2024.04.01.587617 (2024).
- 29. Goncharov, M. et al. VDJdb in the pandemic era: a compendium of T cell receptors specific for SARS-CoV-2. *Nat. Methods* **19**, 1017–1019 (2022).
- Tickotsky, N., Sagiv, T., Prilusky, J., Shifrut, E. & Friedman, N. McPAS-TCR: a manually curated catalogue of pathology-associated T cell receptor sequences. *Bioinformatics* 33, 2924–2929 (2017).
- 31. Klinger, M. et al. Multiplex identification of antigen-specific T cell receptors using a combination of immune assays and immune receptor sequencing. *PLoS ONE* **10**, e0141561 (2015).
- May, D. H. et al. Identifying immune signatures of common exposures through co-occurrence of T-cell receptors in tens of thousands of donors. Preprint at bioRxiv https://doi.org/ 10.1101/2024.03.26.583354 (2024).
- Pesesky, M. et al. Antigen-driven expansion of public clonal T cell populations in inflammatory bowel diseases. J. Crohns Colitis https://doi.org/10.1093/ecco-jcc/jjaf048 (2025).
- Andreu-Sánchez, S. et al. Phage display sequencing reveals that genetic, environmental, and intrinsic factors influence variation of human antibody epitope repertoire. *Immunity* 56, 1376–1392.e8 (2023).
- 35. Vogl, T. et al. Population-wide diversity and stability of serum antibody epitope repertoires against human microbiota. *Nat. Med.* **27**, 1442–1450 (2021).
- 36. Vogl, T. et al. Systemic antibody responses against human microbiota flagellins are overrepresented in chronic fatigue syndrome patients. *Sci. Adv.* **8**, eabq2422 (2024).
- 37. Bourgonje, A. R. et al. Phage-display immunoprecipitation sequencing of the antibody epitope repertoire in inflammatory bowel disease reveals distinct antibody signatures. *Immunity* **56**, 1393–1409.e6 (2023).
- 38. Lindsey, J. W. Antibodies to the Epstein-Barr virus proteins BFRF3 and BRRF2 cross-react with human proteins. *J. Neuroimmunol.* **310**, 131–134 (2017).
- Fechtner, S. et al. Antibody responses to Epstein–Barr virus in the preclinical period of rheumatoid arthritis suggest the presence of increased viral reactivation cycles. Arthritis Rheumatol. 74, 597–603 (2022).
- Ascherio, A. et al. Epstein–Barr virus antibodies and risk of multiple sclerosis: a prospective study. *JAMA* 286, 3083–3088 (2001)
- Pasoto, S. G. et al. EBV reactivation serological profile in primary Sjögren's syndrome: an underlying trigger of active articular involvement? *Rheumatol. Int.* 33, 1149–1157 (2013).

- 42. Leung, A. K. C. et al. Infectious mononucleosis: an updated review. *Curr. Pediatr. Rev.* **20**, 305–322 (2024).
- Robinson, W. H., Younis, S., Love, Z. Z., Steinman, L. & Lanz, T. V. Epstein–Barr virus as a potentiator of autoimmune diseases. *Nat. Rev. Rheumatol.* 20, 729–740 (2024).
- 44. Bjornevik, K. et al. Longitudinal analysis reveals high prevalence of Epstein–Barr virus associated with multiple sclerosis. *Science* **375**, 296–301 (2022).
- 45. Moon, U. Y. et al. Patients with systemic lupus erythematosus have abnormally elevated Epstein–Barr virus load in blood. *Arthritis Res. Ther.* **6**, R295 (2004).
- 46. Whittingham, S., McNeilage, L. J. & Mackay, I. R. Epstein-Barr virus as an etiological agent in primary Sjögren's syndrome. *Med. Hypotheses* **22**, 373–386 (1987).
- 47. Jog, N. R. et al. Association of Epstein–Barr virus serological reactivation with transitioning to systemic lupus erythematosus in at-risk individuals. *Ann. Rheum. Dis.* **78**, 1235 (2019).
- 48. McClain, M. T. et al. Early events in lupus humoral autoimmunity suggest initiation through molecular mimicry. *Nat. Med.* **11**, 85–89 (2005).
- Csorba, K. et al. Anti-C1q antibodies as occurring in systemic lupus erythematosus could be induced by an Epstein–Barr virus-derived antigenic site. Front. Immunol. 10, 2619 (2019).
- Lanz, T. V. et al. Clonally expanded B cells in multiple sclerosis bind EBV EBNA1 and GlialCAM. Nature 603, 321–327 (2022).
- Morrison, T. E., Mauser, A., Wong, A., Ting, J. P.-Y. & Kenney, S. C. Inhibition of IFN-γ signaling by an Epstein–Barr virus immediate-early protein. *Immunity* 15, 787–799 (2001).
- 52. Tsurumi, T., Fujita, M. & Kudoh, A. Latent and lytic Epstein-Barr virus replication strategies. *Rev. Med. Virol.* **15**, 3-15 (2005).

- 53. Salamun, S. G. et al. The Epstein–Barr virus BMRF1 protein activates transcription and inhibits the DNA damage response by binding NuRD. *J. Virol.* **93**, e01070-19 (2019).
- 54. Perdue, C. L., Eick-Cost, A. A. & Rubertone, M. V. A brief description of the operation of the DoD serum repository. *Mil. Med.* **180**, 10–12 (2015).
- 55. Ebert, A. C. et al. Risk of inflammatory bowel disease following hospitalisation with infectious mononucleosis: nationwide cohort study from Denmark. *Nat. Commun.* **15**, 8383 (2024).
- Liu, W. et al. Structures of capsid and capsid-associated tegument complex inside the Epstein–Barr virus. *Nat. Microbiol.* 5, 1285–1298 (2020).

Publisher's note Springer Nature remains neutral with regard to jurisdictional claims in published maps and institutional affiliations.

Open Access This article is licensed under a Creative Commons Attribution 4.0 International License, which permits use, sharing, adaptation, distribution and reproduction in any medium or format, as long as you give appropriate credit to the original author(s) and the source, provide a link to the Creative Commons licence, and indicate if changes were made. The images or other third party material in this article are included in the article's Creative Commons licence, unless indicated otherwise in a credit line to the material. If material is not included in the article's Creative Commons licence and your intended use is not permitted by statutory regulation or exceeds the permitted use, you will need to obtain permission directly from the copyright holder. To view a copy of this licence, visit https://creativecommons.org/licenses/by/4.0/.

© The Author(s) 2025

Institute of Clinical Molecular Biology, Kiel University and University Hospital Schleswig-Holstein (UKSH), Kiel, Germany. ²Adaptive Biotechnologies, Seattle, WA, USA. 3Center for Cancer Research, Medical University of Vienna, Vienna, Austria. 4Norwegian PSC Research Center, Department of Transplantation Medicine, Division of Surgery and Specialized Medicine Oslo University Hospital Rikshospitalet, Oslo, Norway. 5 Research Institute of Internal Medicine, Oslo University Hospital, Oslo, Norway. 6 Institute of Clinical Medicine, University of Oslo, Oslo, Norway. 7 Departments of Neurology, Biomedicine and Clinical Research, and Research Center for Clinical Neuroimmunology and Neuroscience Basel (RC2NB), University Hospital Basel and University of Basel, Basel, Switzerland. *Department of Biomedicine, Infection Biology Laboratory, University and University Hospital Basel, Basel, Switzerland. 9Department of Internal Medicine I, Division of Hepatology/Transplant Hepatology, University Hospital Schleswig-Holstein, Kiel, Germany. 10 Popgen Biobank and Institute of Epidemiology, University of Kiel, Kiel, Germany. 11 Institute of Transfusion Medicine, University Hospital Schleswig-Holstein, Lübeck/Kiel, Kiel, Germany. 12 Institute of Medical Informatics and Statistics, Kiel University and University Hospital Schleswig-Holstein, Kiel, Germany. 13 Department of General, Visceral-, Thoracic-, Transplant- and Pediatric-Surgery, University Hospital Schleswig-Holstein Campus Kiel, Kiel, Germany. 14 Hybrid Technology Hub-Centre of Excellence, Institute of Basic Medical Sciences, Faculty of Medicine, University of Oslo, Oslo, Norway. 15 Institute of Immunology, University of Kiel, Kiel, Germany. 16 Department of Internal Medicine, University Medical Center Hamburg-Eppendorf, Hamburg, Germany. 17 University Transplant Center, University Medical Center Hamburg-Eppendorf, Hamburg, Germany. 18Department of Internal Medicine I, University Hospital of Bonn, Bonn, Germany. 19Department of Gastroenterology, Hepatology and Oncology, Vivantes Humboldt-Hospital, Berlin, Germany. 20 Department of Gastroenterology, Hepatology Infectious Diseases and Endocrinology, Hannover Medical School, Hannover, Germany. 21Interdisciplinary Crohn Colitis Centre Minden, Minden, Germany. 22Department of Pathology, University Medical Center Schleswig-Holstein, Kiel, Germany. 23 Division of Infectious Diseases, University and University Hospital Basel, Basel, Switzerland. 24 Center of Neurology, Department of Neuroimmunology, University Hospital and University Bonn, Bonn, Germany. 25 German Center for Neurodegenerative Diseases (DZNE), Bonn, Germany. 26First Department of Medicine, University Medical Centre Hamburg Eppendorf, Hamburg, Germany. 27Martin Zeitz Center for Rare Diseases, University Medical Centre Hamburg-Eppendorf, Hamburg, Germany. 28 Hamburg Centre for Translational Immunology (HCTI), University Medical Center Hamburg-Eppendorf, Hamburg, Germany. Me-mail: a.franke@ikmb.uni-kiel.de

Methods

Ethical approval

The study was approved by the ethical committee at the University of Kiel under the following ethical votes: D441/16, D474/12, A161/08, A103/14 and A148/14, and by the Regional Committees for Medical and Health Research Ethics of South-Eastern Norway (reference numbers 18221 and 13381). Written informed consent was collected from all participants before the beginning of the study. For isolating monoclonal antibodies from liver samples, fresh PSC and PBC liver explants were collected at Queen Elizabeth Hospital in Birmingham, UK and at Oslo University Hospital Rikshospitalet in Oslo, Norway. As per the Declaration of Helsinki, written informed consent was obtained from participants in accordance with local research ethics committee approvals in Birmingham (LREC no. 06-Q2702-61) and Regional Committees for Medical and Health Research Ethics of South-Eastern Norway (reference numbers 13381, 18221 and 15368).

Study cohorts

PSC samples were collected from three tertiary referral centers across Germany, namely the University Medical Center Hamburg-Eppendorf, Hannover Medical School and Charité-Berlin University Medicine. Detailed clinical information related to these samples is shown in Extended Data Table 1. The samples used for TCR-seq (n = 504) were collected from 2008 to 2020, whereas the serum samples utilized for PhIP-seq measurements (n = 120) were collected from 2015 to 2021 primarily at the University Medical Center Hamburg-Eppendorf. Recruitment of participants and collection of biomaterials was coordinated through the biobank popgen (https://portal.popgen.de/). Specifically, popgen sent blank study sets to most of the recruiting clinics. The clinic included study participants and sent the biomaterials and questionnaires back to popgen. The study set contained blood sample kits, a questionnaire and an informed consent form. In some other cases, participants were asked by the clinic to take part in the study and subsequently contacted popgen to receive the study set. Healthy controls were derived from age- and sex-matched healthy blood donors (Extended Data Table 1) collected at the Institute of Transfusion Medicine through support of the Institute of Clinical Molecular Biology at the University Medical Center Schleswig-Holstein (UKSH). Samples included in the TCR-seq analysis (n = 904) were obtained from 2015 to 2017, whereas samples included in the PhIP-seq analysis (n = 202)were collected from 2016 to 2017.

TCR profiling

Genomic DNA was extracted from frozen, plasma-depleted blood samples using the Qiagen DNeasy Blood Extraction Kit (Qiagen). As much as 18 μg of input DNA was then used to perform immunosequencing of the CDR3 regions of TCR- β (TRB) chains, that is the TRB repertoire, using the immunoSEQ assay (Adaptive Biotechnologies). Briefly, input DNA was amplified in a bias-controlled multiplex PCR, followed by high-throughput sequencing 16 . Sequences were collapsed and filtered to identify and quantify the absolute abundance of each unique TRB CDR3 region for further analyses 57 . To estimate the proportion of T cells out of total nucleated cells input for sequencing, or T cell fraction, a panel of reference genes present in all nucleated cells was amplified simultaneously 58 .

Clonotype processing and filtration

We started by removing nonproductive clonotypes. Subsequently, we combined DNA rearrangement that yielded the same protein rearrangement together by summing their count and estimated frequency. Given the redundancy in the codon, different CDR3 nucleotide sequences will encode the same CDR3 amino acid sequence. Thus, we combined rearrangement with the same CDR3 protein sequence and different nucleotide sequences together as the protein sequence is the only relevant part for recognizing antigens presented by HLA proteins.

Identifying PSC-associated clonotypes

PSC-associated clonotypes were identified using an incidence-based analytical framework ¹⁷. First, we extracted public clonotypes, that is, clonotypes present in two or more people. For each public clonotype, we compared its frequency, that is its prevalence or occurrence, in the PSC and the healthy cohort using a one-sided Fisher's exact test. Consequently, we utilized a permutation-based method ¹⁷ to estimate the false discovery rate and the significance threshold for the association test. We considered any clonotype with a Fisher's exact P value $< 9 \times 10^{-5}$ (< 5% false discovery rate) to be PSC-associated. When comparing the repertoire of individuals with PSC with the repertoire of individuals with CD or UC, we used the same framework except that we used a two-sided Fisher's exact test, then permutations were used to generate an analysis-tailored P value cutoff for a false discovery rate < 5%.

Seeded clustering of disease-associated clonotypes

To increase the number of disease-associated clonotypes, we developed a two-step clustering algorithm:

- (1) Clustering based on the sequence similarity.

 Here we used the amino acid sequence of the CDR3 to calculate the Levenshtein distance between each unique pair of PSC-associated clonotypes and all TRB clonotypes identified in our study cohort. Next, we selected pairs that have a Levenshtein distance of one, that is, clonotypes with higher sequence divergence were dropped from subsequent processing steps. The result of this step was a map between each PSC-associated clonotype and a collection of highly similar clonotypes that differ in their CDR3 sequence by one Levenshtein distance.
- (2) Clusters purification.
 - To avoid introducing noise into the identified meta-clonotypes that were generated in step (1) based on sequence similarity only, we filtered the list of clonotypes present in a meta-clonotype by calculating the association strength in terms of P value between the seed and each member of the meta-clonotype. If the PSC-association P value of the seed and the candidate clonotype in the meta-cluster of the seed, was lower than the PSC-association P value of the seed only, then we assume that this candidate clonotype is also associated with PSC but because it has a lower frequency in the population, in other words lower prevalence, it was not associated with PSC in the main analysis using the Fisher's exact test. Nonetheless, if the calculated PSC-association P value was higher than the seed, we assume that this candidate clonotype is just a noise that is not associated with PSC. For each candidate clonotype in each meta-cluster identified in step (1), this filtration criterion is applied to removes noise introduced by sequence similarity and not by similarity in response, enabling us to identify a collection of highly similar clonotype sequences that are implicated in PSC.

Global screening array genotyping and HLA imputation

We genotyped 431 people with PSC and 773 controls using the single nucleotide polymorphism global screening array from Illumina. Subsequently, classical HLA-I and HLA-II alleles were imputed at the two-field resolution, that is four-digits resolution, from these genotypes 59,60 .

Generation of the TCR-seq validation datasets

Two datasets were used to validate the identified PSC-associated clonotypes. The first was derived from the SPARC IBD cohort of the Crohn's and Colitis Foundation IBD Plexus program²⁵. The TRB repertoires of these people were profiled using the immunoSEQ assay (Adaptive Biotechnologies) similar to the TRB repertoires of the discovery cohort. The second validation dataset was derived from 64 healthy controls

and 154 people with PSC from Oslo University Hospital, Norway. For these samples, RNA was extracted from PAXgene tubes. Subsequently, 200 ng of RNA was used to profile the T cell repertoire using the Human TCR RNA Multiplex kit with UMI (MiLaboratories) following the manufacturer's protocol. After sample demultiplexing, MIXCR (v.4.6.0)⁶¹ was used for identifying TRB clonotypes from the generated sequencing reads.

Pathogen enrichment analysis

The analysis was performed using a hypergeometric test that accommodates four different variables, the total number of clonotypes, the number of clonotypes successfully annotated in a given database and the total number of clonotypes available for a particular pathogen in the database. Finally, the number of clonotypes annotated to be derived from a particular pathogen. Clonotypes with multiple antigenic specificities in the annotation database were dropped before the enrichment analysis.

ECOCluster clonotype burden

ECOClusters are generated from TCRs with a known HLA association³², allowing us to ignore some instances of TCR cross-reactivity between HLAs. When calculating the clonotype burden for the ECOCluster TCRs, we counted clonotypes that are associated with HLAs encoded by the sample donor. We then divided this count by the total number of clonotypes observed in the sample to reach the ECOCluster burden.

PhIP-seq immunoprecipitation, library preparation and sequencing

As a first step and to ensure a uniform antibody input for immunoprecipitation, each serum sample IgG antibody concentration was measured by a standard sandwich enzyme-linked immunosorbent assay (ELISA; primary antibody: goat anti-human IgG-UNLB, SB-2040-01; secondary antibody: goat F(ab')2 anti-human IgG-HRP, SB-2042-05). Three antigen libraries were used for performing PhIP-seq, namely, a microbiota library containing 244,000 variants³⁵ a library composite of 100,000 peptides derived from environmental and allergic proteins⁶² and a library containing 13,192 antigenic peptides from different corona viral antigens⁶³. The optimal ratio of phages and antibodies per reaction was determined beforehand and seemed to be a 4,000-fold coverage of phages per variant and 2 µg of antibodies³⁵. First, a 96-deep-well plate (Greiner Bio-One, cat. no. 780270) was blocked with PhIP-seq blocking buffer (980 µl, Dulbecco's phosphate-buffered saline (DPBS) with 3% BSA and 0.05% Tween 20) overnight at 4 °C on a rotator. Phages were then resuspended in extraction buffer (20 mM Tris-HCl, 100 mM NaCl, 6 mM MgSO₄, pH 8.0, with 2 g I^{-1} BSA) to ensure a 4,000-fold coverage per variant. Resuspended phages were centrifuged for 2 h at 4 °C, at 3,000g to remove any cell debris or precipitate that could interfere with the assay. Bacteriophages (980 µl) were transferred to the preblocked 96-deep-well plate. Serum IgG antibodies (2 µg) were added to the bacteriophages. The plate was sealed with a 96-well sealing mat (Axygen, cat. no. AM-2ML-SQ) and incubated overnight at 4 °C on a rotator. A full-skirted 96-well PCR plate (Azenta Framestar, cat. no. 4ti-0960/W) preblocked with 150 µl of PhIP-seq blocking buffer (DPBS with 3% BSA and 0.05% Tween 20) overnight at 4 °C was prepared for the washing step. Protein A/G-coated magnetic beads (1:1 mixture of Invitrogen Dynabeads Protein A, cat. no. 10008D and Protein G, cat. no. 10009D) were washed three times with magnetic beads wash buffer (DPBS with 0.02% Tween 20) and resuspended in DPBS. Beads (40 μ l) were added to bacteriophage-antibody mixtures, the plate was sealed with a 96-well sealing mat, and incubated for 4h at 4 °C on a rotator to ensure peptide-antibody complex formation. After 4 h, the plate was centrifuged at 900g for 2 min at room temperature before removing most of the supernatant. Beads were resuspended in the leftover (~100 μl) volume and transferred to the preblocked 96-well PCR plate. Beads were then washed twice with 145 µl of immunoprecipitation wash buffer (50 mM Tris-HCl, 150 mM NaCl, 0.1% IGEPAL CA630, pH 7.5). After the last wash step, the supernatant was removed, and the beads were stored at -20 °C until further processing. For pooled Illumina amplicon sequencing, several PCRs were performed with Q5 polymerase (New England Biolabs, cat. no. M0493L) according to the manufacturer's recommendations. The following primer pairs were used: for PCR1, tcgtcg-gtctcgtgggctcggagatgtgtataagagacagATGCTCGGGGATCCGAATTC; for PCR2, 10-nt unique dual index primers purchased from IDT; for PCR3 (of PCR2 pools), AATGATACGGCGACCACCGA and CAAGCAGAAGACG-GCATACGA). PCR3 products were cut from an agarose gel and purified twice (1×QIAquick gel extraction kit, cat. no. 28704; 1×QIAquick PCR purification kit, cat. no. 28106; both according to manufacturer's manual). Sequencing was done on an Illumina NovaSeg machine (custom primers for R1: ttactcgagtgcggccgcaagctttca; for R2: tgtgtataagagacagatgctcggggatccgaattct; R1/R244/31 nt).

PhIP-seq data preprocessing

Pooled samples were sequenced with Illumina Novaseq 6000 paired read sequencing with 75 bp (read 1) and 25 bp (read 2). Raw reads were mapped to all three antigen libraries 35,62,63, and the counts per peptide were normalized by comparing them with the base oligopeptide levels in the initial library (sequenced before immunoprecipitation)³⁵. The generated count matrices were modeled using a generalized Poisson distribution, the two parameters, that is, λ and θ of this distribution, were estimated by analyzing the relationship between number of reads per variants in the library before immunoprecipitation and after immunoprecipitation but without incubation with serum. The probability of observing a particular count of reads against a particular antigen in the combined bacteriophage library was calculated using the fitted generalized Poisson model. Finally, Bonferroni correction was used to corrected for multiple testing. Subsequently, the fold-change of normalized peptide counts was computed to measure the level of enrichment. Information about fold-change levels, adjusted P values, read counts and presence-absence scores for each peptide were saved in separate matrix-like tables and used for downstream analysis. Before the association analysis, we filtered out samples with less than 250 bound antigens as well as samples with more than 3,000 antigens, because samples with either a very high or a very low number of bound-antigens might bias our statistical analyses.

Isolation of liver-infiltrating mononuclear cells

Liver-infiltrating mononuclear cells (LIMCs) were isolated from liver tissue collected from recipient liver explants collected after liver transplantation⁶⁴. Briefly, 50-100-g tissue sections were cut into 1-2 mm³ pieces, washed three to four times with PBS and resuspended in digestion media (RPMI 1640, 3% FBS, collagenase type 1A (VWR International)) for 30 min at 37 °C. Digested tissue was homogenized mechanically using a Stomacher 400 circulator (Seward) and washed repeatedly with PBS through 63 µm nylon filters. Washed tissue was discarded and filtered cell suspensions were spun at 600g for 5 min. Wash supernatant was discarded and cell pellets were washed an additional three to four times with PBS to remove debris. Following the final wash, cell pellets were resuspended in PBS, and LIMCs were isolated by density centrifugation using Lympholyte-H (Cedarlane). Collected LIMCs were pelleted, resuspended in CryoStor cryopreservation medium (Sigma-Aldrich) at 5-25 × 106 cells per aliquot, and stored in liquid nitrogen.

Enrichment of hepatic B cells for single-cell RNA sequencing

Frozen LIMC aliquots were thawed quickly in 37 °C RPMI 1640 supplemented with 5% FBS and washed to remove cryopreservation medium. LIMCs were counted and resuspended at the recommended concentration for EasySep human Pan B cell negative-bead enrichment (StemCell Concentration for EasySep human Pan B cell negative-bead enrichment).

Technologies), and B cells were enriched following the manufacturer's protocol. To remove dead and dying cells postenrichment, B cells were stained with live/dead Zombie NIR dye (BioLegend) and sorted using a FACSMelody (BD Biosciences) before single-cell VDJ B cell receptor sequencing.

Single-cell VDJ B cell receptor sequencing, alignment and annotation

Single-cell VDJ B cell receptor sequencing (BCR-seq) was performed on sorted liver B cells using Chromium Next GEM Single Cell 5'Library kit v.1.1 (10x Genomics) following the manufacturer's user guide CG000207 Rev E. Pooled BCR cDNA libraries were barcoded, multiplexed and sequenced on a NovaSeq (Illumina) SP 200 cycle flow cell at 5,000 read pairs per cell. Sequencing reads were demultiplexed, aligned and annotated to the human genome reference GRCh38 (GENCODE v.32/Ensembl98) using Cell Ranger v.6.1.2 (10x Genomics) and BCR-seq was analyzed using Loupe VDJ Browser v.4.0.0 (10x Genomics).

Generation of monoclonal antibodies

CDR3 BCR sequences obtained from single-cell VDJ BCR-seq were synthesized into monoclonal antibodies using high throughput (HTP-gene-to-antibody production service (GenScript)). Briefly, CDR3 sequences of expanded B cell clonotypes were cloned into pcDNA3.4 plasmids coexpressing human IgG1 kappa or human IgG1 lambda and transfected into the HD293F mammalian expression system. Monoclonal antibodies were purified using AmMag Protein A magnetic beads and resuspended in PBS and 50% glycerol for long-term storage.

Antigen-specific T cell enrichment with HLA-B*08:01 tetramers

Freshly isolated or thawed peripheral blood mononuclear cells (PBMC) from HLA-B*08-positive healthy donors and people with PSC were blocked with anti-FcR reagent (Miltenyi) and stained first with a mix of PE-labeled HLA-B*08:01 tetramers loaded with RAKFKQLL (BZLF1) and FLRGRAYGL (EBNA3) peptides (immunAware APS). Samples were further stained with a cocktail of antibodies including anti-CD4-BV510 (clone OKT4, BioLegend), anti-CD8a-BV711 (clone RPA-T8, BioLegend), anti-CD3-BV785 (clone UCHT1, BioLegend), anti-CCR7-BV421 (clone G043H7, BioLegend), anti-CD45RA-Pe/Cy7 (clone HI100, BioLegend) and a live/dead dye 7AAD. Antigen-specific CD8+T cells were gated as 7AAD-CD8+CD3+tetramer+ and sorted directly into RLT lysis buffer (Qiagen) using the SONY MA900 cell sorter.

In vitro stimulation for induction of CD137 expression and antigen-specific CD8 T cell enrichment

Freshly isolated PBMCs were plated in 24-well plate at density of 7×10^6 cells per well in 1 ml RPMI 1640, supplemented with 5% FCS and 1% penicillin-streptomycin. PepTivators EBV BZLF1 and EBNA1 (Miltenyi) consisting of 15-mer peptides covering EBV's BZLF1 and EBNA1 proteins were used as antigens either separately (at peptide concentration 0.6 μ M each) or as mix (at peptide concentration 0.3 μ M each). Negative control wells without antigen stimulation were set for each donor and processed in parallel. After 16 h of incubation at 37 °C in 5% CO₂, cells were harvested, stained with anti-CD137-PE antibody (clone 4B4-1, Miltenyi) and labeled further with anti-PE magnetic microbeads (Miltenyi). Antigen-specific CD137+ cells were enriched with positive magnetic selection on MS-columns (Miltenyi). CD137+ enriched cells were stained on columns with an antibody cocktail including anti-CD4-BV510 (clone OKT4, BioLegend), anti-CD8a-BV711 (clone RPA-T8, BioLegend), anti-CD3-BV785 (clone UCHT1, BioLegend), anti-CCR7-BV421 (clone G043H7, BioLegend), anti-CD45RA-Pe/Cy7 (clone HI100, BioLegend), anti-CD69-FITC (clone FN50, BioLegend) and a live/dead dye 7AAD. Afterwards, the on-column staining cells were eluted from the columns and sorted on SONY MA900 cell sorter. Antigen-specific CD8⁺T cells were gated as 7AAD⁻CD8⁺CD137⁺CD69⁺

and sorted directly into RLT lysis buffer (Qiagen). Negative control wells were analyzed in parallel.

Profiling the TRB repertoire of EBV-specific clonotypes

RNA was extracted from tetramer-sorted antigen-stimulated T cells using the RNeasy Micro Kit (Qiagen, cat. no. 74104). All extracted RNA was used to profile the TRB repertoire using the Human TCR RNA Multiplex kit with UMI (MiLaboratories) following the manufacturer's protocol. Prepared libraries were sequenced using an Illumina NextSeq 1000 P1 lane (2 \times 150 bp), generating approximately 100 million reads, providing an average of 7–7.7 million reads per library. After sample demultiplexing, MiXCR (v.4.6.0) 61 was used for identifying TRB clonotypes from the generated sequencing reads.

Generation and cultivation of EBV-transformed LCLs and EBV-specific T cell lines

To generate EBV-transformed lymphoblastoid cell lines (LCLs), frozen PBMCs were thawed from selected individuals with PSC (n = 4), centrifuged at 300g for 5 min at 4 °C in RPMI 1640 (Gibco), containing 10% heat-inactivated FCS (Gibco) and 1% penicillin-streptomycin (PenStrep; Gibco), and B cells were negatively selected using a Pan B isolation kit (Miltenyi). B cells were treated with CpG ODN 2006 (InvivoGen) and EBV supernatant for 1.5 h at 37 °C, 5% CO₂. Next, the B cells were cultured with irradiated healthy donor feeder cells in medium consisting of RPMI 1640 (Gibco), 1% penicillin-streptomycin (PenStrep; Gibco), 5% human AB serum, 2% GlutaMAX (Gibco), 1% Minimum Essential Medium Non-Essential Amino Acids (Gibco) and 1% sodium pyruvate (Gibco), in addition to 1.25 µg ml⁻¹CpG ODN 2006 at 37 °C, 5% CO₂. During expansion, the medium was replaced, and the cells were split as needed. To generate EBV-specific T cell lines, flowthrough from the negatively $selected\,B\,cells\,was\,used\,according\,to\,the\,manufacturer's\,instructions.$ Cells were expanded in CTL medium (CTL-M) comprising of RPMI 1640 (Sigma-Aldrich), 1% penicillin-streptomycin (PenStrep; Gibco) and 10% human AB serum, supplemented with IL-4 (400 U ml⁻¹), IL-7 (10 ng ml⁻¹) and 0.1 µg ml⁻¹ peptide pools: EBV consensus (Miltenyi), EBV-BZLF1, EBV-BMRF1 and EBV-EBNA1 (all JPT Peptide Technologies). Cells were pulsed with peptides in 1 ml in a 24-well G-Rex device (Wilson Wolf) overnight, then supplemented with CTL-M containing IL-4 and IL-7, and cultured for 14 days. Next, EBV-specific T cell lines were harvested and further expanded for 14 days in CTL-M containing irradiated T2 cells, irradiated PBMCs and 30 ng ml⁻¹ OKT-3. The next day, 50 U ml⁻¹ IL-2 was added, and again every third day. On day 4, culture medium was replaced completely, and medium was changed subsequently as needed. After 14 days of T2 expansion, T cell lines were frozen down in CTL-M containing 20% dimethyl sulfoxide (Sigma-Aldrich).

Interferon-y ELISpot

To investigate the antigenic response of EBV-specific T cell lines, expanded T cell lines were thawed and $3\times10^5\,\mathrm{T}$ cells were added to anti-interferon- γ -coated (1 mg ml $^{-1}$; clone 1-D1K, Mabtech) ELISpot MultiScreen $_{\rm HTS}$ 96-well filter plates (Merck). T cells were stimulated overnight with autologous EBV-LCLs in an effector:target (E:T) ratio of 1:1 and allogenic HLA-B:08-matched EBV-LCLs and nontransformed B cells in an E:T ratio of 5:1. Allogenic HLA-B:08-matched donors were used due to limited material. Plates were developed using interferon- γ antibody (Mabtech), streptavidin-alkaline phosphatase (Mabtech), and 1-Step NBT/BCIP (Thermo Fisher Scientific). Spots were counted on dried plates with an AID ELISpot Reader.

TriNetX

The TriNetX US Collaborative Network provides access to anonymized electronic medical records of 116 million people, from 65 US health-care organizations. Medical health records of people <80 years of age from the US collaborative network were used to assemble cohorts of people diagnosed with infectious mononucleosis, excluding those

who had also been diagnosed with *Chlamydia*, and people diagnosed with *Chlamydia* but not infectious mononucleosis. Propensity score matching for sex and age at the index between the two cohorts resulted in 124,383 people per cohort. We chose *Chlamydia* for negative control matching as it presents with a similar age distribution to that of infectious mononucleosis. Analytics for cohort outcomes, including people with outcome before the time window, were performed on the TriNetX Live Advanced Analytics dashboard with only aggregate results from infectious mononucleosis and control cohorts being surfaced and returned to the platform.

Protein structural localization of BFRF3 in the EBV capsid

The EBV capsid reconstruction from cryogenic electron microscopy was retrieved from the Protein Databank (PDB ID 6w19) 56 and visualized with Mol* 3D-Viewer. For analyzing the BFRF3/MCP hexon complex only, chains A–F (MCP) and Q–V (BFRF3) were extracted from the PDB file and visualized with PyMOL.

Statistics and reproducibility

We used a cross-sectional study design in which we profiled the immune repertoire of people with PSC and healthy controls. Sample size for this study was based on availability considerations, as we did not recruit new participants but used stored biomaterial from previously recruited people with PSC and healthy blood donors. To have sufficient power to detect even small effects, we used biomaterial of all individuals with PSC that were available to us and of a larger number of healthy blood donors. The available sample sizes of n = 504 individuals with PSC and n = 904 healthy controls provide at least 95% power to detect differences of $d \ge 0.2$ (standardized effect size) with a Mann-Whitney test (G*Power v.3.1). We also performed PhIP-seq on 120 people with PSC and 202 people without PSC. Some samples were removed during the quality control of the assays, mainly from the PhIP-seq dataset (those with fewer than 250 bound antigens or more than 3,000 bound antigens); no other metrics were used to exclude samples from any of these analyses. PSC-associated clonotypes were identified using a one-sided Fisher's exact test and the association between infectious mononucleosis and time to PSC onset in the TriNetX dataset was calculated using the Cox proportional hazard model. Pathogen enrichment analysis was conducted using the hypergeometric test. Independent groups (for example, individuals with PSC versus healthy controls or carriers versus noncarriers of specific HLA alleles) were compared regarding different quantitative variables (for example, burden of PSC-associated clonotypes) by the two-sided nonparametric Mann–Whitney–Wilcoxon test as most variables were expected to be skewed and non-Gaussian. Association between such quantitative variables (for example, number of unique clonotypes and burden of PSC-associated clonotypes) was assessed by the nonparametric Spearman correlation coefficient.

Reporting summary

Further information on research design is available in the Nature Portfolio Reporting Summary linked to this article.

Data availability

The TCR-seq results of 904 healthy participants and 504 participants with PSC are available via Zenodo at https://doi.org/10.5281/zenodo.14989127 (ref. 65). The PhIP-seq data of participants with PSC are available via Zenodo at https://doi.org/10.5281/zenodo.14989837 (ref. 66) and for healthy controls at https://doi.org/10.5281/zenodo.14989788 (ref. 67). Due to GDPR and consent restrictions, clinical data from these people can be obtained by submitting a project application to the popgen v.2.0 Network (https://portal.popgen.de/) with a processing time of approximately 2 months. The first validation dataset, namely, the US-based SPARC IBD dataset, is available upon approved application to the Crohn's and Colitis Foundation IBD Plexus Program (https://www.crohnscolitisfoundation.org/ibd-plexus).

Regarding the second validation dataset containing the TRB repertoire of people with PSC as well as healthy controls from Norway, institutional data privacy regulations prohibit deposition of individual level data to public repositories. Participant written consent also does not cover public sharing of data for use for unknown purposes. Upon contact with T.H.K. (t.h.karlsen@medisin.uio.no) an institutional data transfer agreement can be established and data shared if the aims of data use are covered by ethical approval and patient consent. The procedure will involve an update to the ethical approval as well as review by legal departments at both institutions, and the process will typically take 1–2 months from initial contact.

References

- Gittelman, R. M. et al. Longitudinal analysis of T cell receptor repertoires reveals shared patterns of antigen-specific response to SARS-CoV-2 infection. *JCI Insight* 7, e151849 (2022).
- 58. Pruessmann, W. et al. Molecular analysis of primary melanoma T cells identifies patients at risk for metastatic recurrence. *Nat. Cancer* **1**, 197–209 (2020).
- Degenhardt, F. et al. Construction and benchmarking of a multi-ethnic reference panel for the imputation of HLA class I and II alleles. Hum. Mol. Genet. 28, 2078–2092 (2019).
- Degenhardt, F. et al. Trans-ethnic analysis of the human leukocyte antigen region for ulcerative colitis reveals shared but also ethnicity-specific disease associations. *Hum. Mol. Genet.* 30, 356–369 (2021).
- 61. Bolotin, D. A. et al. MiXCR: software for comprehensive adaptive immunity profiling. *Nat. Methods* **12**, 380–381 (2015).
- 62. Leviatan, S. et al. Allergenic food protein consumption is associated with systemic IgG antibody responses in non-allergic individuals. *Immunity* **55**, 2454–2469.e6 (2022).
- 63. Klompus, S. et al. Cross-reactive antibodies against human coronaviruses and the animal coronavirome suggest diagnostics for future zoonotic spillovers. Sci. Immunol. **6**, eabe9950 (2021).
- 64. Chung, B. K. et al. Phenotyping and auto-antibody production by liver-infiltrating B cells in primary sclerosing cholangitis and primary biliary cholangitis. *J. Autoimmun.* **77**, 45–54 (2017).
- ElAbd, H. et al. The TRB repertoires for ElAbd et al.; 2025; Nat Med. Zenodo https://doi.org/10.5281/zenodo.14989127 (2025).
- ElAbd, H. et al. The PhIP-Seq repertoires of the 120 individuals with PSC from ElAbd et al.; 2025; Nat Med manuscript. Zenodo https://doi.org/10.5281/zenodo.14989837 (2025).
- 67. ElAbd, H. et al. The PhIP-Seq repertoires of the 202 healthy controls from ElAbd et al.; 2025; Nat Med manuscript. *Zenodo* https://doi.org/10.5281/zenodo.14989788 (2025).

Acknowledgements

We would like to thank N. Braun, M. E. Figuera Basso, A. Tanck, X. Yi and M. Gozhenko for their help with preparing the DNA samples. We would also like to thank T. Wesse and M. Wittig for helping with genotyping and R. Kraemer, J. Fuß and S. Franzenburg for the technical support during the sample preparation. Further, we would like to thank A.-C. Lecourt for technical support in generating EBV Bcell lines and C. Makowiec for providing the EBV supernatant. We thank E. Liaskou and L. Brynjulfsen for their help with generating the monoclonal antibodies. We are grateful to the Crohn's and Colitis Foundation IBD Plexus program for providing us with the Tcell repertoire profiles of the SPARC IBD cohort. The project was funded by the EU Horizon Europe Program grant miGut-Health: personalized blueprint of intestinal health (101095470; award to A.F.) and the EU program for Research and Innovation 'Horizon Health' (HORIZON-HLTH-2023-DISEASE-03) ID-DarkMatter-NCD (897856542; award to T.V.). Additionally, the project received funding from the Deutsche Forschungsgemeinschaft (DFG, German Research Foundation) Research Unit 5042: 'miTarget—The Microbiome as a

Therapeutic Target in Inflammatory Bowel Diseases' (award to A.F.), along with funding from the Cluster of Excellence 2167 'Precision Medicine in Chronic Inflammation (PMI)' (award to S.S.). The project was further funded by a Swiss National Science Foundation (SNSF) Eccellenza Fellowship (194609), an SNSF Starting Grant (211318) as well as funding from the State Secretariat for Education, Research and Innovation SERI (24.00020) as part of the EU program for Research and Innovation 'Horizon Health' (HORIZON-HLTH-2023-DISEASE-03) ID-DarkMatter-NCD (897856542) (all to A.-K.P.). The funding agencies had no role in the design, collection, analysis and interpretation of data or in writing the manuscript. The SPARC IBD cohort is maintained by the Crohn's and Colitis Foundation for research use.

Author contributions

A.F., H.E., T.H.K., C. Schramm, C.R., S.S., B.H., H.S.R., T.V., A.D., F.T., P.B. and B.H. designed and conceived the study. H.E., M.P., G.I., D.H.M. and A.K.H.M. conducted the secondary TCR-seq and PhIP-seq analyses. G.M. performed structural analysis on the PhIP-seq results. M.V.H. analyzed the medical records of people with PSC. A.K.H.M., M.P., T.A.S. and V.K. conducted experimental work to analyze the EBV signal in the immune repertoire of people with PSC and controls. L.K., A.-K.P., D.S., C. Stühler and N.K. performed function experiments and produced cell lines to quantify the anti-EBV response in people with PSC. B.K.C. produced monoclonal antibodies from PSC livers. A.K.H.M., E.R., S.M., W.L. M.Z., F.B., R.G., T.F., J.R.H., E.M., M.S., T.J.W., H.L., S.S. and B.B. helped with study participant recruitment and sample collection. H.E. wrote the first draft of the manuscript with subsequent contributions from all co-authors.

Funding

Open access funding provided by Christian-Albrechts-Universität zu Kiel.

Competing interests

M.P., D.H.M., B.H. and H.S.R. have or had employment and equity ownership with Adaptive Biotechnologies. H.E. did an internship at Adaptive biotechnologies from July 2023 until September 2023. F.T. received speaker's fees from Abbvie, Bristol-Myers-Squibb, Celltrion Healthcare, Dr Falk Pharma, Eli Lilly, Ferring Pharmaceuticals and Janssen, and funding from Sanofi/Regeneron. T.H.K. declares consulting fees from Albireo, Boehringer Ingelheim, MSD, Gilead and Falk Pharma unrelated to the present work. A.-K.P. (institution) has received speaker, consulting or travel honoraria from Novartis, Biogen, Roche and UCB all used for research support and unrelated to the present work. The other authors declare no competing interests.

Additional information

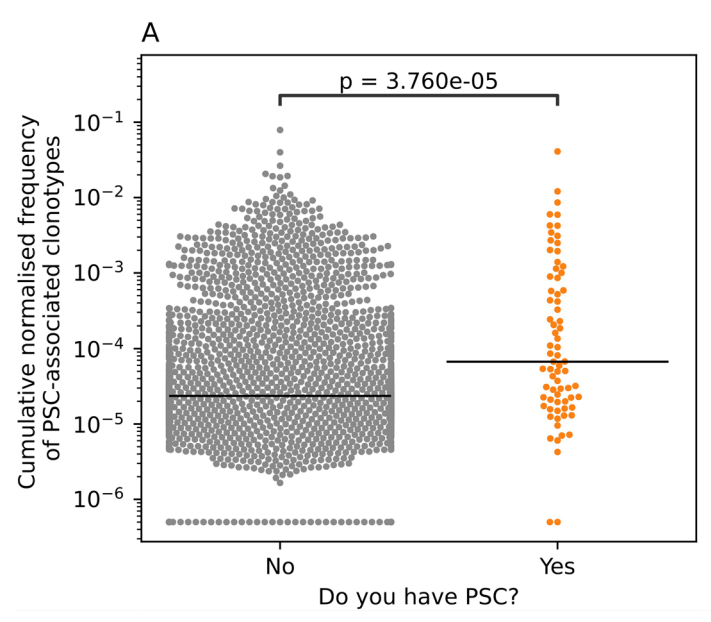
Extended data is available for this paper at https://doi.org/10.1038/s41591-025-03692-w.

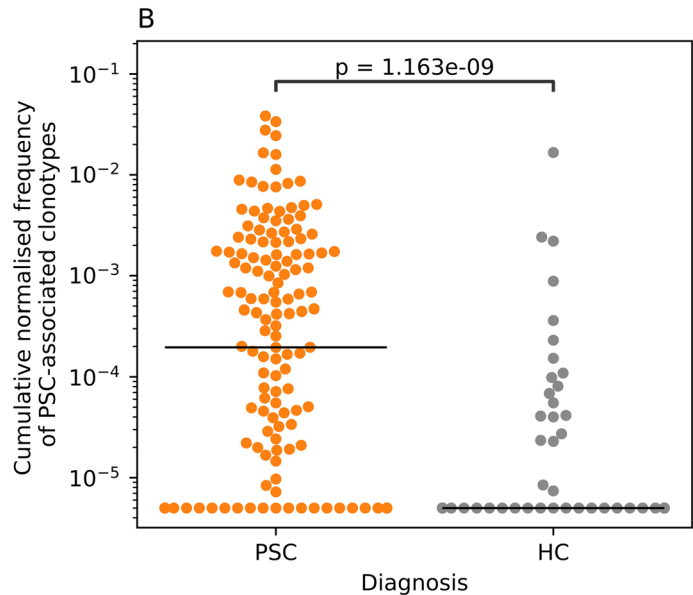
Supplementary information The online version contains supplementary material available at https://doi.org/10.1038/s41591-025-03692-w.

Correspondence and requests for materials should be addressed to Andre Franke.

Peer review information *Nature Medicine* thanks David Assis, Klemens Ruprecht and the other, anonymous, reviewer(s) for their contribution to the peer review of this work. Primary Handling Editor: Sonia Muliyil, Lia Parkin and Liam Messin, in collaboration with the *Nature Medicine* team.

Reprints and permissions information is available at www.nature.com/reprints.

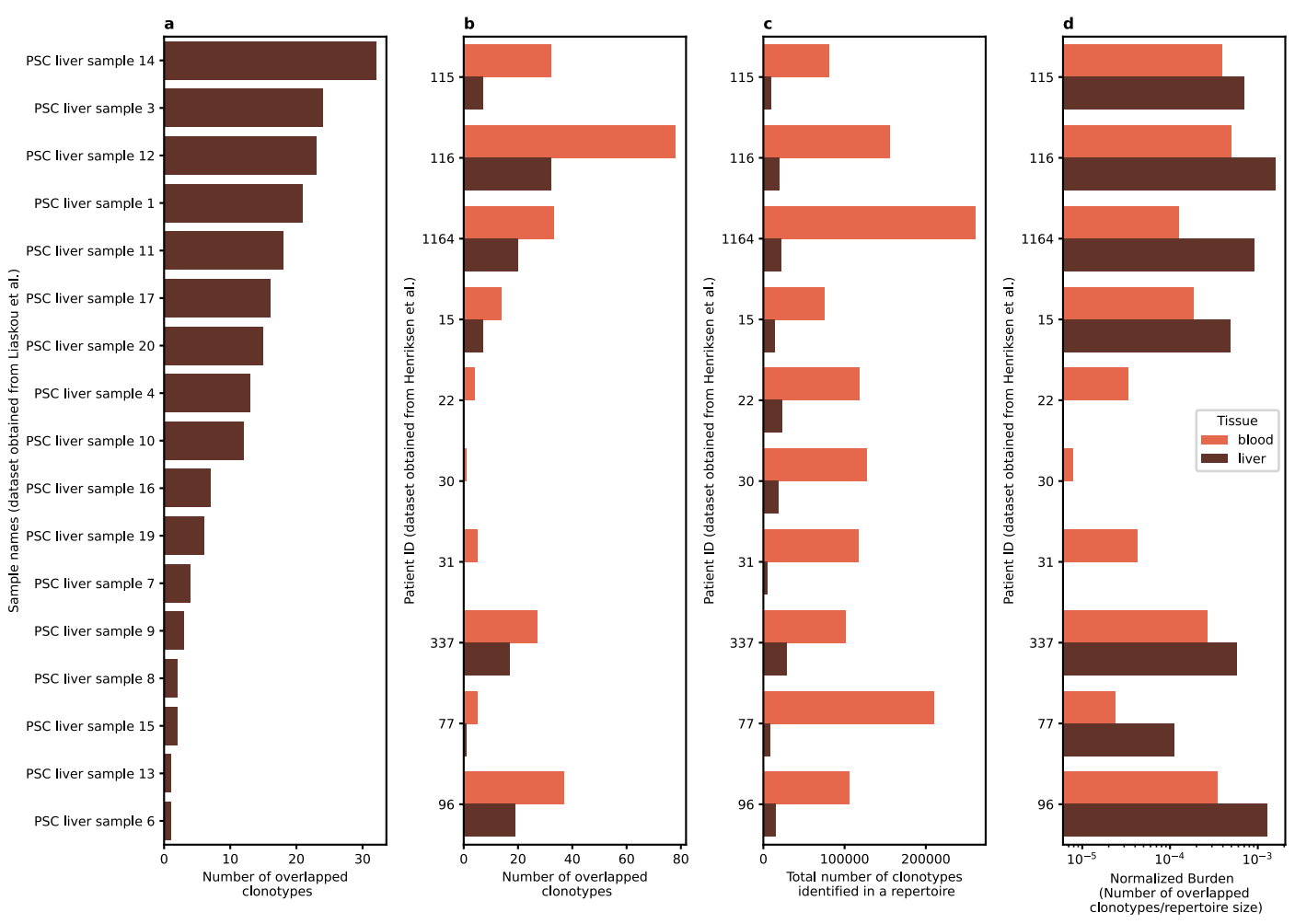




 $Extended \ Data \ Fig.\ 1 \ |\ The\ expansion\ of\ the\ 1,008\ PSC\ -associated\ clonotypes\ identified\ in\ the\ current\ study\ in\ two\ independent\ validation\ cohorts.$

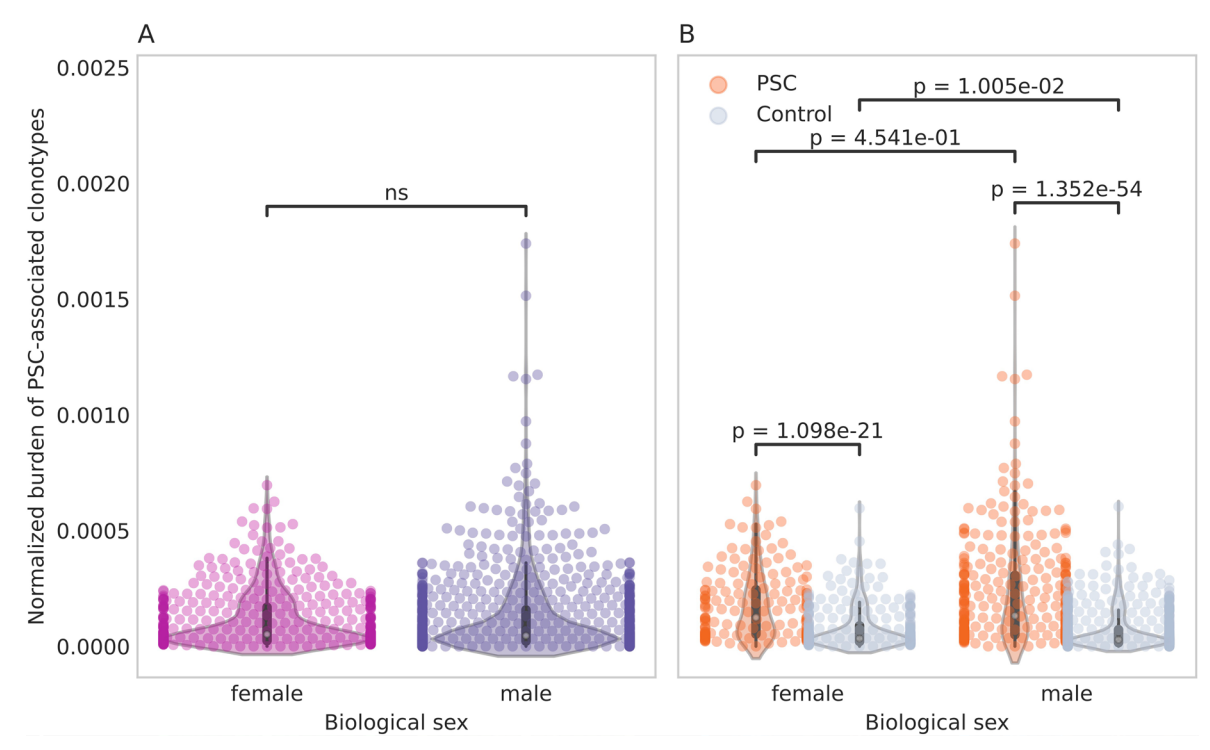
(a) The expansion of the PSC-associated clonotypes in the US-based SPARC IBD cohort containing 2,487 individuals with IBD and 73 individuals with PSC-IBD²⁵. (b) The expansion of PSC-associated clonotypes in 154 individuals with PSC and

64 healthy controls from Norway. Each dot represents the cumulative expansion of all PSC-associated clonotypes in the repertoire of an individual, and the black lines represent the median. In both panels, a two-sided Mann-Whitney-Wilcoxon test was used to compare the expansion of PSC-associated clonotypes.



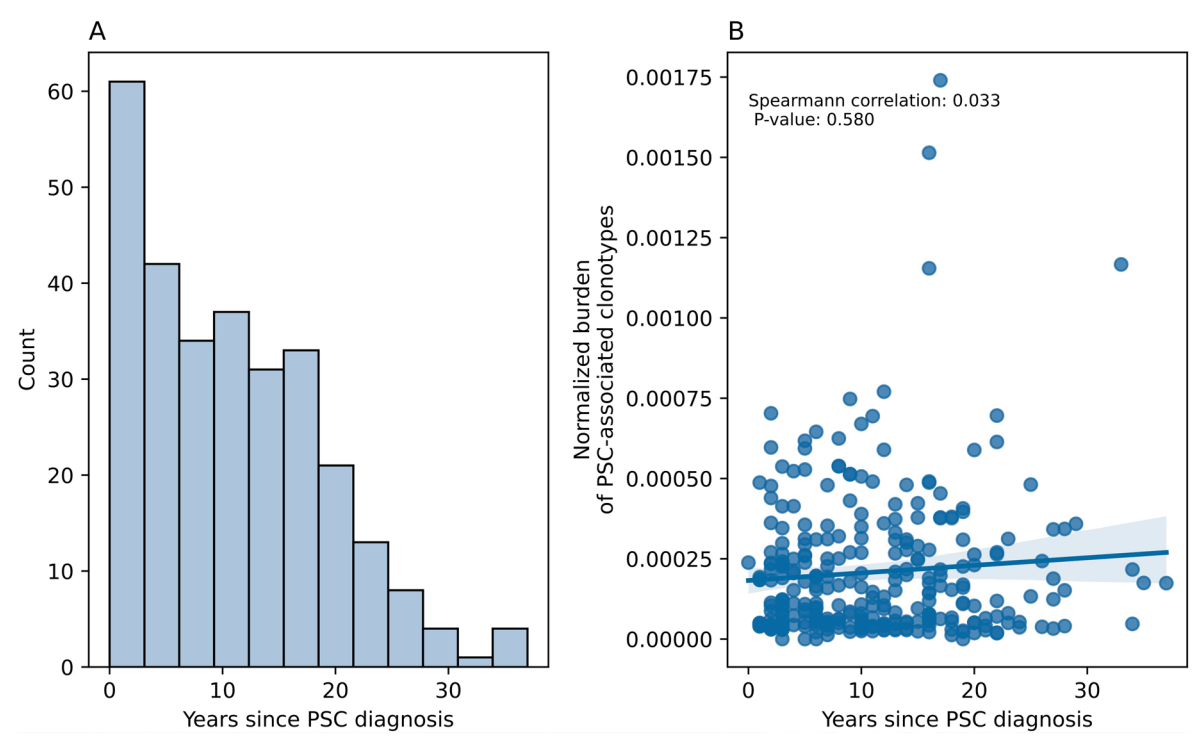
Extended Data Fig. 2 | The identified 1,008 PSC-associated clonotypes are detected and expanded in PSC livers. (a) The number of PSC-associated clonotypes that were detected in different PSC-liver repertoires. The PSC liver TRB repertoires were obtained from Liaskou $et\,al.^{26}$. (b) shows the number of PSC-associated clonotypes that were detected in the blood and liver repertoires

of individuals with PSC. (\mathbf{c}) depicts the total number of unique clonotypes identified in the blood and liver of each individual in the utilized dataset. (\mathbf{d}) illustrates the normalized burden of PSC-associated clonotypes in the liver as well as blood of people with PSC. The dataset used in (\mathbf{b}), (\mathbf{c}), and (\mathbf{d}) is derived from Henriksen *et al.*²⁷.



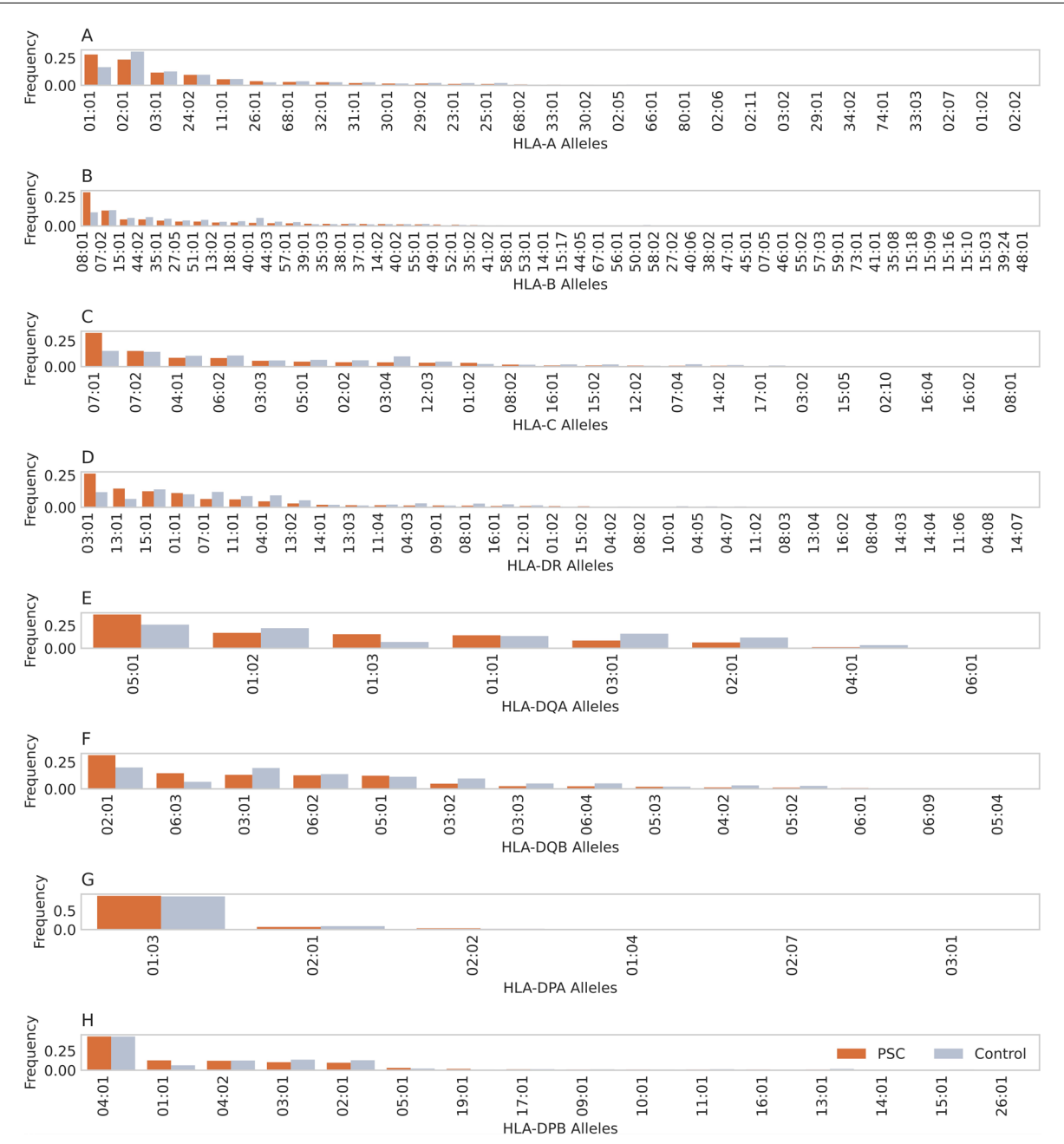
Extended Data Fig. 3 | **The normalized burden of PSC-associated clonotypes is not associated with biological sex.** (a) The lack of difference in the normalized burden in females (n = 471 individuals) relative to males (n = 937 individuals) irrespective of the underlying disease across the entire cohort of PSC and healthy controls. (b) The burden of PSC-associated clonotypes was significantly higher in individuals with PSC relative to healthy controls independent of the biological sex. This analysis was performed across the entire cohort which contains 304 females without PSC, 167 females with PSC, 600 males without PSC and 337

males with PSC. In both panels, each dot represents the cumulative expansion of all PSC-associated clonotypes in the repertoire of an individual, black lines represent the median across different individuals, the boxplots represent the interquartile range (IQR) and the whiskers represent datapoints within the 1.5 times the IQR range. Lastly, a two-sided Mann-Whitney-Wilcoxon test was used to compare the normalized burden across the different groups included in the study.



Extended Data Fig. 4 | The relationship between the burden of PSC-associated clonotypes and years since PSC-diagnosis. (a) The distribution of years since diagnosis across the cohort. (b) The correlation between years since PSC

diagnosis and the normalized burden of PSC-associated clonotypes. In both panels, the TRB repertoires of 289 individuals with PSC was included in the analysis.

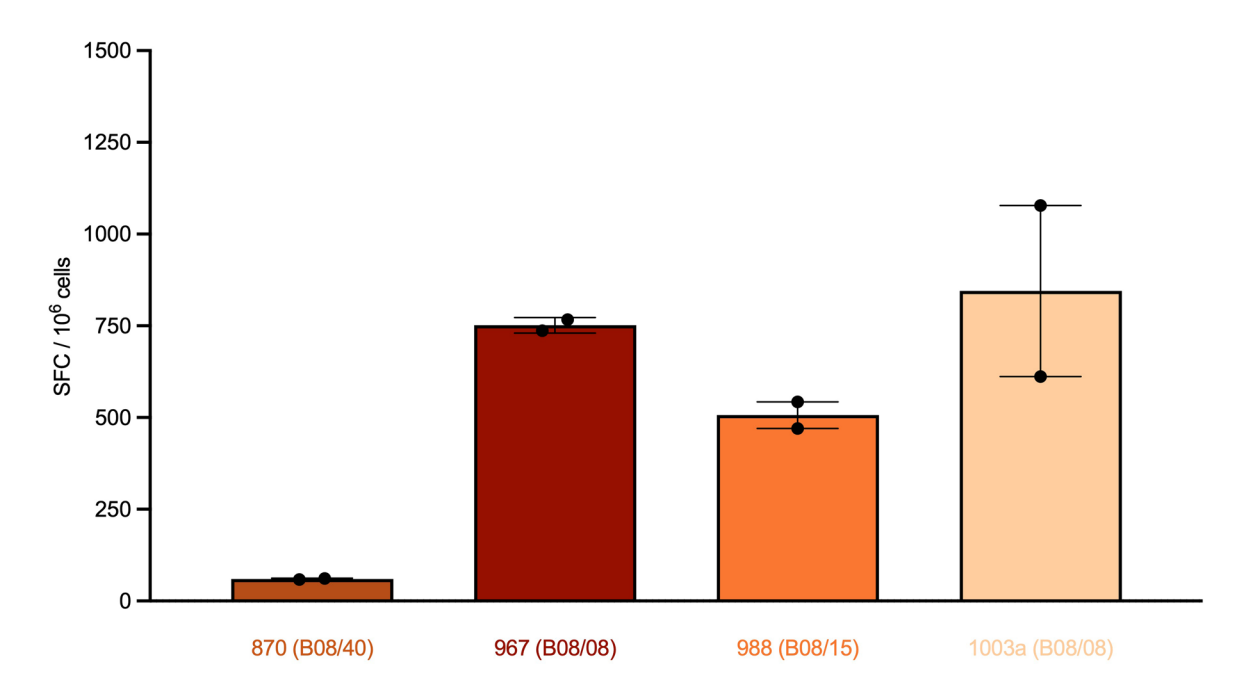


Extended Data Fig. 5 | The frequency of different HLA alleles in the discovery cohort of individuals with PSC and healthy controls. (a) The frequency of HLA-A alleles in the PSC cohort and the healthy cohort. (b), (c), (d), (e), (f), (g) and (h), The frequency of HLA-B alleles, HLA-DRB1 alleles, HLA-DRB1 alleles, HLA-DRB1

alleles, HLA-DQB1 alleles, HLA-DPA1 alleles and HLA-DPB1 alleles in the PSC cohort and the healthy cohort, respectively. In all panels, the imputed HLA alleles from genotyping arrays for 431 individuals with PSC and 773 individuals without PSC were analyzed.



Response against autologous LCLs



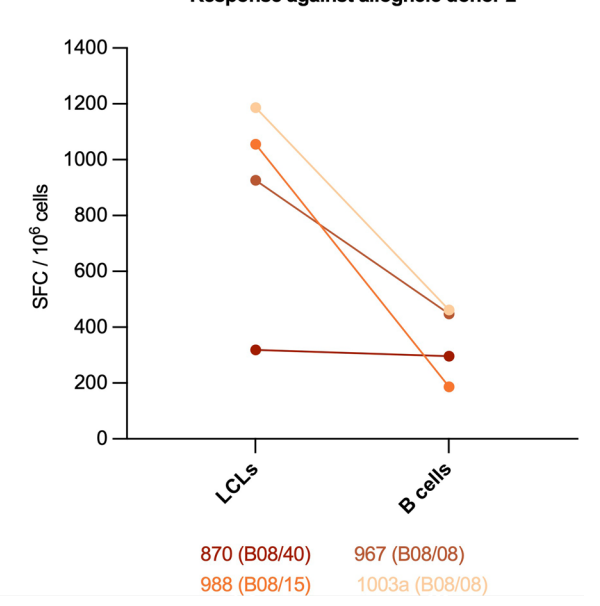


Response against allogneic donor 1

1400 — 1200 — 10

Extended Data Fig. 6 | EBV-specific response of expanded T cell lines against EBV-LCLs and non-transformed B cells in IFN-gamma ELISpot. Response of T cell lines from individuals with PSC (n = 4) towards autologous Epstein-Barr virus lymphoblastoid cell lines (EBV-LCLs) in an effector:target (E:T) ratio of 1:1 (a) or against EBV-LCLs and non-transformed B cells in E:T ratio of 5:1 from two partially

Response against allogneic donor 2



HLA-matched allogenic donors (**b**). Plotted values represent the mean and standard deviation of the spot-forming colonies (SFC) per 10° cells subtracted by the spot-forming colonies (SFC) per 10° cells of the unstimulated T cell controls (negative controls ranging from 0-7 SFC/ 10° cells) of two technical replicates.

 $\textbf{Extended Data Table 1} \ \textbf{The clinical and phenotypic properties of the study cohort included in the TCR sequencing experiment} \\$

		PSC	Controls
	Number of samples	504	904
Basic information	Percentage of males	67%	67%
	A (μ=43.67±12.73	μ=44.69±13.52
	Age (years)	Med=43.0	Med=47.0
		Yes (n=64; 12.7%)	NA
	Liver- transplantation	No (n=252; 50%)	NA
		Unknown (n=188; 37.30%)	NA
		Yes (n=29; 5.75%)	NA
	cholecystitis	No (n=212; 42%)	NA
		Unknown (n=263; 52.2%)	NA
		Yes (n=47; 9.3%)	NA
	cholecystectomy	No (n=42; 8.33%)	NA
	joine services and the services are services are services and the services are s	Unknown (n=415;82.34%)	NA
	cholangiocarcinoma	Yes (n=20; 4%)	NA
Comorbidities		No (n=193; 38.3%)	NA
	onorang.coaromoma	Unknown (n=291; 57.7%)	NA
		Yes (n=244; 48.4%)	NA
	 IBD	No (n=127; 25.2%)	NA
		Unknown (n=133; 26.4%)	NA
	IBD subtype	UC (n=167; 33.1%)	NA
		CD(n=33;6.54%)	NA
		IBD-U (n=13; 2.57%)	NA
		IBD-S (n=8; 1.587) [suspension of IBD]	NA
		Unknown (n= 283; 56.15%)	NA

nature portfolio

Corresponding author(s):	Hesham ElAbd, Andre Franke
Last updated by author(s):	Mar 6, 2025

Reporting Summary

Nature Portfolio wishes to improve the reproducibility of the work that we publish. This form provides structure for consistency and transparency in reporting. For further information on Nature Portfolio policies, see our <u>Editorial Policies</u> and the <u>Editorial Policy Checklist</u>.

For all statistical analyses, confirm that the following items are present in the figure legend, table legend, main text, or Methods section.

_				
ι.	+~	+ 1	-	ics
`	ıa		\sim 1	11 \

n/a	Confirmed
	$oxed{\boxtimes}$ The exact sample size (n) for each experimental group/condition, given as a discrete number and unit of measurement
	🔀 A statement on whether measurements were taken from distinct samples or whether the same sample was measured repeatedly
	The statistical test(s) used AND whether they are one- or two-sided Only common tests should be described solely by name; describe more complex techniques in the Methods section.
	A description of all covariates tested
	🔀 A description of any assumptions or corrections, such as tests of normality and adjustment for multiple comparisons
	A full description of the statistical parameters including central tendency (e.g. means) or other basic estimates (e.g. regression coefficient) AND variation (e.g. standard deviation) or associated estimates of uncertainty (e.g. confidence intervals)
	For null hypothesis testing, the test statistic (e.g. <i>F</i> , <i>t</i> , <i>r</i>) with confidence intervals, effect sizes, degrees of freedom and <i>P</i> value noted <i>Give P values as exact values whenever suitable.</i>
\boxtimes	For Bayesian analysis, information on the choice of priors and Markov chain Monte Carlo settings
\boxtimes	For hierarchical and complex designs, identification of the appropriate level for tests and full reporting of outcomes
\boxtimes	Estimates of effect sizes (e.g. Cohen's <i>d</i> , Pearson's <i>r</i>), indicating how they were calculated
	Our way collection on statistics for higherite contains articles on many of the points above

Software and code

Policy information about availability of computer code

Data collection

No software were used for data collection.

Data analysis

Data analysis was mainly conducted using different Python 3 libraries and frameworks such as Pandas (1.5.3), SciPy (1.13.0) and NumPy (1.25.2) in addition to miXCR (v4.6.0). Data visualization was also conducted using Matplotlib (3.8.0) and Seaborn (0.11.2). For BCR-Seq data analysis, Cell Ranger v.6.1.2 (10X Genomics) and Loupe VDJ Browser v4.0.0 (10X Genomics) were used.

For manuscripts utilizing custom algorithms or software that are central to the research but not yet described in published literature, software must be made available to editors and reviewers. We strongly encourage code deposition in a community repository (e.g. GitHub). See the Nature Portfolio guidelines for submitting code & software for further information.

Data

Policy information about availability of data

All manuscripts must include a data availability statement. This statement should provide the following information, where applicable:

- Accession codes, unique identifiers, or web links for publicly available datasets
- A description of any restrictions on data availability
- For clinical datasets or third party data, please ensure that the statement adheres to our policy

The TCR-seq results of 904 healthy participants and 504 participants with PSC are available via Zenodo at https://doi.org/10.5281/zenodo.14989127. The PhIP—seq data of participants with PSC are available via Zenodo at https://doi.org/10.5281/zenodo.14989837 and for healthy controls at https://doi.org/10.5281/zenodo.149898837 and for healthy con

zenodo.14989788. Due to GDPR and consent restrictions, clinical data for these people can be obtained by submitting a project application to the popgen v.2.0 Network (https://portal.popgen.de/) with a processing time of approximately 2 months. The first validation dataset, namely, the US-based SPARC IBD dataset, is available upon approved application to the Crohn's and Colitis Foundation IBD Plexus Program (https://www.crohnscolitisfoundation.org/ibd-plexus). Regarding the second validation dataset containing the TRB repertoires of people with PSC as well as healthy controls from Norway, institutional data privacy regulations prohibit deposition of individual level data to public repositories. Participant written consent also does not cover public sharing of data for use for unknown purposes. Upon contact with T.H.K. (t.h.karlsen@medisin.uio.no) an institutional data transfer agreement can be established and data shared if the aims of data use are covered by ethical approval and patient consent. The procedure will involve an update to the ethical approval as well as review by legal departments at both institutions, and the process will typically take 1–2 months from initial contact.

Research involving human participants, their data, or biological material

Policy information about studies with <u>human participants or human data</u>. See also policy information about <u>sex, gender (identity/presentation)</u>, and sexual orientation and race, ethnicity and racism.

Reporting on sex and gender

We utilized large-scale immune-repertoire profiling data using TCR-Seq for 504 individuals with PSC and 904 controls. In addition, we performed PhIP-Seq on 120 samples and 202 healthy controls. For the TCR-Seq cohorts, we had a male ratio of 67% to reflect the male-predominance observed in the individuals with PSC (here also 67%). For samples measured with PhIP-Seq we had a 47% and 57% males in the PSC and control samples, respectively. Self-reported sex was previously validated using SNP-array-based sex predictions for the same samples. We studied sex-specific effects in the burden analysis of disease-associated clonotypes shown in Extended Data Figure 3 where the burden of PSC-associated clonotypes was comparable in individuals with PSC and and in controls.

Reporting on race, ethnicity, or other socially relevant groupings

There was no reporting on race or ethnicity on the study, as most samples were collected from individuals with European-ancestry.

Population characteristics

The population characteristics are described in table S1. In brief, samples used for TCR-Seq had the following characteristics:

- 1. Age mean=43.67±12.73 for PSC patients and 44.69±13.52 for healthy controls.
- 2. both sample panels had an equal ratio of males and females with 67% of the cohorts being male For samples included in PhIP-Seq analysis, the study population had the following properties
- 1. median age= 44.65 ±13.24 for PSC and 46.8±8.47 for healthy controls
- 2. 47.5% of the PSC cohort consisted of males and 57% of the controls were male

Recruitment

Healthy controls were recruited via the local transfusion medicine department from blood donors, while individuals with PSC were recruited via the local biobank PopGen. For the current study, we have not actively recruited participant but used stored biomaterial from previously recruited PSC patients and healthy blood donors. The samples were selected to have matching age and sex distribution whenever possible.

Ethics oversight

The study has been approved by the ethical committee at the University of Kiel under the following ethical votes: D441/16, D474/12, A161/08, A103/14, and A148/14. Also, by the Regional Committees for Medical and Health Research Ethics of South-Eastern Norway (reference numbers 18221 and 13381). A written informed consent was collected from all participants prior to the beginning of the study. For isolating monoclonal antibodies from liver samples, fresh PSC and PBC liver explants were collected at Queen Elizabeth Hospital in Birmingham, United Kingdom, and at Oslo University Hospital Rikshospitalet in Oslo, Norway. As per the Declaration of Helsinki, written informed consent was obtained from participants in accordance with local research ethics committee approvals in Birmingham (LREC #06-Q2702-61) and Regional Committees for Medical and Health Research Ethics of South-Eastern Norway (reference numbers 13381, 18221 and 15368).

Note that full information on the approval of the study protocol must also be provided in the manuscript.

Field-specific reporting

Р	lease select the one below that is	the best fit for your research.	If you are not sure, read t	the appropriate sections be	efore making your selection.

X Life sciences

Behavioural & social sciences Ecological, evolutionary & environmental sciences

For a reference copy of the document with all sections, see <u>nature.com/documents/nr-reporting-summary-flat.pdf</u>

Life sciences study design

All studies must disclose on these points even when the disclosure is negative.

Sample size

Sample size for this study was based on availability considerations, as we did not recruit new individuals but used stored biomaterial from previously recruited individuals with PSC and healthy blood donors. In order to have sufficient power to detect even small effects, we used biomaterial of all individuals with PCS that were available to us and of a larger number of healthy blood donors. The available sample sizes of n=504 individuals with PSC and n=904 healthy controls provide at least 95% power to detect differences of d>=0.2 (standardized effect size) with a Mann-Whitney test (G*Power 3.1).

Data exclusions

While some samples were removed during the quality control of these assays, mainly from the PhIP-Seq dataset were samples with fewer than 250 bound antigens or more than 3,000 bound antigens we removed, no other metrics was used to exclude samples from any of these analyses.

Replication

We replicated our findings at the T cell repertoire level using two independent datasets. First, the "A Study of a Prospective Adult Research

Replication	(Cohort with IBD" cohort of the US-based Crohn's & Colitis Foundation IBD Plexus program (SPARC IBD) which contains 2,487 individuals with IBD only and 73 individuals with PSC-IBD. Second, a PSC cohort from Norway that contains 154 individuals with PSC and 64 healthy controls.		
Randomization	We utilized a cross-sectional study design where we profiled the immune repertoire of individuals with PSC and healthy controls. Healthy controls were selected to match the age and sex distribution of individuals with PSC whenever possible.		
Blinding	Given our case-control study, blinding was only used during data generation where samples from healthy controls and individuals with PSC were randomized and barcoded.		
Reportin	g for specific materials, systems and methods		
	on from authors about some types of materials, experimental systems and methods used in many studies. Here, indicate whether each material, ted is relevant to your study. If you are not sure if a list item applies to your research, read the appropriate section before selecting a response.		
Materials & exp	perimental systems Methods		
n/a Involved in th	ne study n/a Involved in the study		
Antibodies	ChIP-seq		
Eukaryotic	cell lines		
Palaeontol	logy and archaeology MRI-based neuroimaging		
Animals an	nd other organisms		
Clinical dat	ra		
Dual use re	esearch of concern		
ı			
Antibodies			
Antibodies used	anti-CD4-BV510 (clone OKT4, biolegend), anti-CD8a-BV711 (clone RPA-T8, biolegend), anti-CD3-BV785 (clone UCHT1, biolegend), anti-CCR7-BV421 (clone G043H7, biolegend), anti-CD45RA-Pe/Cy7 (clone HI100, biolegend), anti-CD137-PE antibody (clone 4B4-1, Miltenyi), anti-IFN-γ-coated (1 mg/ml; clone 1-D1K, Mabtech), Goat Anti-Human IgG-UNLB (SB-2040-01), Goat F(ab')2 Anti-Human IgG-HRP (SB-2042-05)		
Validation	1. the validation of anti-CD4-BV510 (https://www.biolegend.com/en-ie/products/purified-anti-human-cd4-antibody-3650? GroupID=BLG590) 2. the validation of anti-CD8a-BV711 (https://www.biolegend.com/en-gb/products/brilliant-violet-711-anti-human-cd8a-		
	antibody-7929) 3. the validation of anti-CD3-BV785 (https://www.biolegend.com/fr-fr/products/brilliant-violet-785-anti-human-cd3-antibody-14454?GroupID=BLG5900)		
	4. the validation of anti-CCR7-BV421 (https://www.biolegend.com/fr-lu/products/brilliant-violet-421-anti-human-cd197-ccr7-antibody-7497)		
	5. the validation of anti-CD45RA-Pe/Cy7 (https://www.biolegend.com/de-at/products/pe-cyanine7-anti-human-cd45ra-antibody-7055?GroupID=GROUP658)		
	6. the validation of anti-CD137-PE antibody (clone 484-1, Miltenyi) (https://www.miltenyibiotec.com/DE-en/products/cd137-		
	antibody-anti-human-4b4-1.html#conjugate=vio-bright-fitc:size=100-tests-in-200-ul) 7. the validation of anti-IFN-γ-coated (1 mg/ml; clone 1-D1K, Mabtech) (https://www.mabtech.com/products/anti-human-ifn-g-mab-1-d1k-unconjugated-3420-3)		
	8. the validation of Goat Anti-Human IgG-UNLB (https://www.southernbiotech.com/goat-anti-human-igg-unlb-2040-01) 9. the validation of Goat F(ab')2 Anti-Human IgG-HRP (https://www.southernbiotech.com/goat-f-ab-2-anti-human-igg-hrp-2042-05)		

Eukaryotic cell lines

Policy information	about call li	nec and Sev and	Gandar in Rasparch

olicy information about <u>cell lines</u>	and Sex and Gender in Research
Cell line source(s)	EBV-transformed lymphoblastoid cell line and EBV-specific T cell lines were generated from PBMC isolated from four individuals with PSC according to the protocol described in the online methods.
Authentication	Cells were not authenticated as B cells are not viable after weeks if they are not EBV transformed so the fact that they spontaneously proliferate after weeks indicates their transformation
Mycoplasma contamination	cell lines tested negative for mycoplasma contamination
Commonly misidentified lines (See ICLAC register)	NA

Plants

Seed stocks

Report on the source of all seed stocks or other plant material used. If applicable, state the seed stock centre and catalogue number. If plant specimens were collected from the field, describe the collection location, date and sampling procedures.

Novel plant genotypes

Describe the methods by which all novel plant genotypes were produced. This includes those generated by transgenic approaches, gene editing, chemical/radiation-based mutagenesis and hybridization. For transgenic lines, describe the transformation method, the number of independent lines analyzed and the generation upon which experiments were performed. For gene-edited lines, describe the editor used, the endogenous sequence targeted for editing, the targeting guide RNA sequence (if applicable) and how the editor was applied.

Authentication

Describe any authentication procedures for each seed stock used or novel genotype generated. Describe any experiments used to assess the effect of a mutation and, where applicable, how potential secondary effects (e.g. second site T-DNA insertions, mosiacism, off-target gene editing) were examined.